Geochemistry and geochronology of the Imbicuí Complex, Western Dom Feliciano Belt, Brazil: Tonian adakite-like subduction-related rocks

Rosemeri Soares Siviero, Edinei Koester, Luis Alberto Dávila Fernandes, Delphine Bosch, Olivier Bruguier, Daniel Triboli Vieira, Rodrigo Chaves Ramos, Gustavo Kraemer

Geochemistry and geochronology of the Imbicuí Complex, Western Dom Feliciano Belt, Brazil: Tonian adakite-like subduction-related rocks

Rosemeri Soares Siviero [a], Edinei Koester [b,*], Luis Alberto Dávila Fernandes [b], Delphine Bosch [c], Olivier Bruguier [c], Daniel Triboli Vieira [b], Rodrigo Chaves Ramos [d], Gustavo Kraemer [e]

[a] Programa de Pós-Graduação em Geociências, Universidade Federal do Rio Grande do Sul, Bento Gonçalves Avenue 9500, 91500-000, Porto Alegre, Rio Grande do Sul, Brazil
[b] Instituto de Geociências, Universidade Federal do Rio Grande do Sul, Bento Gonçalves Avenue,9500, 91501-970, Porto Alegre, Rio Grande do Sul, Brazil
[c] Laboratoire de Tectonophysique, UMR/CNRS 5568, Université de Montpellier II, 34095, Montepellier, Cedex 05, France
[d] Secretaria de Meio Ambiente e Preservação Ecológica, Prefeitura Municipal de Sapiranga, João Corrêa Avenue, 800, 93800-222, Sapiranga, Rio Grande do Sul, Brazil
[e] MSc. Geologist, Universidade Federal do Rio Grande do Sul, Brazil

ARTICLE INFO

Keywords:
HSA adakite
Eclogite
Tonian
Dom Feliciano Belt
São Gabriel Terrane
Juvenile accretion

ABSTRACT

Dioritic-tonalitic-trondhjemitic metamorphic rocks represent the Imbicuí Complex in Western Dom Feliciano Belt, São Gabriel Terrane, Lavras do Sul region, Brazil. This complex presents rocks with an adakite-like signature showing high Sr contents (573.5–1337 ppm), Sr/Y ratio higher than 64.08, low Y content (< 33.7 ppm), $(La/Yb)_N > 10$, and $Yb_N < 16$ being classified as Type 1, high silica and high-Al_2O_3 adakites. The adakites present a low-K calc-alkaline affinity, with a U–Pb LA-ICP-MS in zircon crystallization age of 828 ± 8 Ma, the product of an eclogitic melting source. Subordinate, metagabbroic rocks occur with tholeiitic affinity, presenting a U–Pb LA-ICP-MS in zircon crystallization age of 845 ± 5 Ma. The adakitic rocks showed $\varepsilon Nd_{(828)}$ (+ 8.2 to + 7.5), model ages Nd-T_{DM} of 0.8 and 0.9 Ga, similar to the age of crystallization, suggesting that these magmas represent juvenile rocks generated in an orogenic environment mixed with reworked rocks (ratios $^{206}Pb/^{204}Pb$ and $^{207}Pb/^{204}Pb$, 17.70 to 18.40 and 15.49 and 15.55) during an oceanic slab melting associated to the closure of Charrua Ocean throughout Tonian in the Western Dom Feliciano Belt.

1. Introduction

Adakites was a term defined by Defant and Drummond (1990) for rocks characterized by a genesis associated with partial melting of young and hot oceanic crust (MORB-like) metamorphosed during increasing prograde metamorphic reactions in basaltic components of the oceanic crust, converted through greenschist amphibolite facies to mineralogies of eclogite facies pressure and temperature, producing mainly diorite-tonalite-trondhjemite magmas.

However, the designation and concepts of adakites have evolved. Their origin is associated with a broad spectrum of rocks generated in an arc environment at different times, ranging from more accepted models such as the primary slab melt to slab melt hybridized by peridotite to melt derived from peridotite metasomatized by slab melt (adakites from France, Rapp et al., 1999; adakites from Japan, Kimura et al., 2014; adakites from the Philippines, Jégo et al., 2005) or as derived from the partial melting of newly under-plated basaltic crust, as suggested by Atherton and Petford (1993) for rocks in the Cordillera Blanca (USA).

More strictly, the term adakite has been postulated to lower mafic crust melting (Central Luzon, Philippines, Yumul et al., 2000), high–P fractionation of water-rich mantle melts, the mixture of evolved melts of mantle magmas recycled in shallow crustal chambers (Castillo, 2012; Ribeiro et al., 2016) or asthenospheric slab window opening, which are adakites generated by the melting of asthenospheric windows below subduction zone (adakites de Baja California, USA, Ribeiro et al., 2016) that in general has a high Nb signature (> 20 ppm) and called Nb-enriched basalts (Defant et al., 1992).

A detailed study classifies adakitic-like rocks in five genetic models (Zhang et al., 2019): i) high silica adakites formed by subduction oceanic crust, ii) low silica adakites formed by mantle melting reacting with silica melts of subducted oceanic crust, iii) high Mg# (HMA) adakitic rocks formed by delamination and consequence interaction with the mantle, iv) oceanic-type (O-type) mainly formed by basaltic under-plating and v) continental-type or potassium-type (C or K-type) formed

* Corresponding author.
E-mail address: koester@ufrgs.br (E. Koester).

by partial melting of the lower crust. All these adakite-like types can be produced in different tectonic settings.

In the Western Domain of the Dom Feliciano Belt, an orogenic belt developed during the configuration of the West Gondwana paleocontinent in the Brasiliano/Pan-African cycle (Hueck et al., 2018; Heilbron et al., 2020), a dioritic-tonalitic-trondhjemitic association is found near Lavras do Sul city, southernmost Brazil. These gabbros, diorites, quartz diorites, tonalites, and dominant trondhjemites were affected by amphibolite facies metamorphism. They were grouped into the Imbicuí Orthometamorphic Suite (Kraemer, 1995) and are nowadays named Imbicuí Complex (Philipp et al., 2018).

Thus, in this contribution, we present a petrological study of Imbicuí Complex rocks using a petrographic, geochemical (whole-rock geochemistry), isotopic (whole-rock Sr-Nd-Pb isotope geochemistry), and geochronological (zircon U–Pb LA-ICP-MS dating) approach. This paper aims to understand the magma sources and processes and the spatial, temporal, and tectonic evolution of the Imbicuí Complex in the Dom Feliciano Belt context during the Brasiliano/Pan-African orogenic cycle.

2. Geological setting

The studied diorite-tonalite-trondhjemite metamorphic rocks outcrop near Lavras do Sul city, in the Western Domain of the Dom Feliciano Belt. This Neoproterozoic orogenic belt represents the southernmost sector of the Mantiqueira Province (Almeida et al., 1981), developed during the configuration of the West Gondwana paleocontinent in the Brasiliano/Pan-African orogenic cycle (Fig. 1A and B), as result of the convergence between several cratons (e.g., Congo, Kalahari, Río de la Plata) and minor blocks/microplates (Hueck et al., 2018; Heilbron et al., 2020). It extends over 1200 km, from Punta del Este, Uruguay, to southernmost Brazil (Sul-rio-grandense Shield in Rio Grande do Sul, and Catarinense Shield, Santa Catarina).

In the Sul-rio-grandense Shield, the Dom Feliciano Belt is subdivided into four main domains based on geophysical and petrotectonic constraints (see reviews in Philipp et al., 2016; Hueck et al., 2018; Ramos et al., 2020 and references therein): i) Western Domain (represented by the São Gabriel Terrane), ii) Central Domain (comprising the Tijucas Terrane and mainly of Camaquã Basin), iii) Eastern Domain (represented by the Pelotas Terrane) and iv) the Southwestern Domain (represented by the Punta del Este Terrane).

These distinct terranes reflect the complex geologic evolution of the Dom Feliciano Belt during the Neoproterozoic, which can be divided into at least four main orogenic stages: Passinho and São Gabriel Orogenies, related to the closure of the Charrua paleo-ocean (e.g., Leite et al., 1998; Saalmann et al., 2011; Arena et al., 2016); Piratini Orogeny, related to the closure of the Charrua paleo-ocean and simultaneous opening of the South Adamastor paleo-ocean (Vieira et al., 2019; Ramos et al., 2020); and Dom Feliciano Orogeny, related to the closure of the South Adamastor paleo-ocean (e.g., Philipp et al., 2016; Bastos et al., 2020; Loureiro et al., 2021).

The metadiorites-tonalites-trondhjemites of Imbicuí Complex are located in the São Gabriel Terrane, which is limited to the west by the Río de la Plata Craton, represented by the ca. 2.4 Ga Santa Maria Chico Granulite Complex (Girelli et al., 2018), and to the east by the Caçapava do Sul suture (western limit of the Tijucas Terrane) (Fig. 1C).

In the São Gabriel Terrane, Tonian oceanic rocks related to the Charrua oceanic basin closed during the Passinho and São Gabriel Orogenies are found in the Palma Accretionary Prism (Arena et al., 2016; Philipp et al., 2016, 2018), comprising metamorphosed slices of oceanic lithosphere and associated meta-volcano sedimentary sequences. Passive margin metasedimentary units are represented by, e.g., the Passo Feio and Arroio Marmeleiro Complexes (e.g., Philipp et al., 2018). Tonian arc-related rocks in this terrane comprise the TTG's of the Passinho Metadiorite (Leite et al., 1998), the orthogneisses, TTG, and metagranitoids of the Imbicuí Orthometamorphic Suite (Kraemer, 1995), and the TTG's of the Cambaí Complex (e.g., Babinski et al., 1996; Leite et al., 1998; Saalmann et al., 2005a, 2005b; Hartmann et al., 2011; Philipp et al., 2018).

The Imbicuí Complex is tectonically interleaved with ophiolitic rocks of the Cerro Mantiqueiras Complex and with rocks of the Cambaí Complex (Hartmann et al., 2019; Siviero et al., 2021). The study area, the Lavras do Sul region (Fig. 2), belongs to the Imbicuí Complex as referred by Philipp et al. (2018) and is represented by Metadiorite Passinho and its association rocks of Tonian age (879 ± 3 Ma, Leite et al., 1998), mainly identified in the previous detailed geological mapping (UFRGS, 2004; 2005). In its southern sector, the metadiorites-tonalites-trondhjemites of this complex are in tectonic contact with quartz-feldspathic metasedimentary rocks of the Arroio Marmeleiro Complex, both intruded by post-orogenic granitoids (Dom Feliciano Orogeny – e.g., Babinski et al., 1996).

3. Analytical methods

Representative fresh samples of the Imbicuí Complex were selected for the petrographic (optical and scanning electron microscopy), geochemical and isotopic (Sr-Nd-Pb) whole-rock analyses, and geochronological (zircon LA-ICP-MS U–Pb dating) investigations.

Whole-rock geochemistry analyses of fourteen samples were powdered to < 200 mesh size in the Núcleo de Preparação de Amostras (NPA), Centro de Estudos em Petrologia e Geoquímica (CPGq), Instituto de Geociências (IGeo) of the Universidade Federal do Rio Grande do Sul (UFRGS), Brazil and analyzed by ICP-MS/OES in Acme Analytical Laboratories Ltd. (Canada).

Two whole-rock samples were analyzed to Sr-Nd-Pb isotopes in a VG Sector 54 Thermal Ionization Mass Spectrometer (TIMS) at the Laboratório de Geologia Isotópica (LGI), CPGq-IGEO-UFRGS. These samples were spiked with mixed $^{87}Rb/^{84}Sr$ and $^{149}Sm/^{150}Nd$ tracers and processed using standard dissolution procedures with HF, HNO_3, and HCl in a Teflon vial warmed on a hot plate until complete material dissolution. Column procedures used cationic AG50W-X8 resin (200–400 mesh) to separate Rb, Sr, and REE, followed by Sm and Nd separation using anionic LN-B50-A resin (100–150 μm). Pb was separated using exchange columns with DOWEX AG-1 X 8 resin (200–400 mesh) eluted with 0.6 N HBr and collected with 6 N HCl. The samples were run in static mode. Rubidium, Sr, Sm, and Pb were run on Re single filaments. Neodymium isotopes were run on Ta-Re-Ta triple filaments. Rubidium was deposited with HNO_3, while Sr, Sm, Nd, and Pb were deposited with H_3PO_4. Neodymium and Sr ratios were normalized to $^{86}Sr/^{88}Sr = 0.1194$ and $^{146}Nd/^{144}Nd = 0.7219$, respectively. Measurements for the Sr NIST standard NBS-987 gave $^{87}Sr/^{86}Sr = 0.710260 \pm 0.000014$, and for the Nd La Jolla, standard values of $^{143}Nd/^{144}Nd = 0.511859 \pm 0.000010$ were obtained. The total procedures blanks for Rb and Sm were < 500 pg, for Sr < 60 pg, for Nd < 150 pg, and for Pb < 100 pg. Typical analytical errors for $^{87}Rb/^{86}Sr$, $^{147}Sm/^{144}Nd$, and $^{206}Pb/^{204}Pb$ ratios are equal to or better than 0.1%. Initial $^{87}Sr/^{86}Sr$ and $^{143}Nd/^{144}Nd$ were calculated using the metatrondhjemite crystallization age (828 Ma) of Imbicuí Complex using the GCDKit program (Janoušek et al., 2006).

U–Pb analyses were performed in zircon of two samples at the Université de Montpellier II (France), using a VG Plasmaquad II ICP spectrometer coupled to a Geolas Q+ platform housing a 193 nm Excimer laser. Zircon crystals from samples were separated using heavy liquid and magnetic techniques at the Laboratório de Separação de Minerais, NPA-CPGq-IGeo-UFRGS, and mounted in epoxy resin together with G91500 standard zircon (Wiedenbeck et al., 1995). Cathodoluminescence and secondary electron images of the selected zircon grains were taken at the LGI-CPGq-IGeo-UFRGS using a JEOL JSM-6610LV scanning electron microscope equipped with a Bruker XFLASH 5030 energy dispersive X-ray spectrometer. Analytical conditions were 15 kV, a spot size of 60 μm, and a working distance of 10 mm. Isotope data were acquired with spot size between 15 and 77 μm, frequency between 3 and 5 Hz, and energy density of 15 J/cm^2.

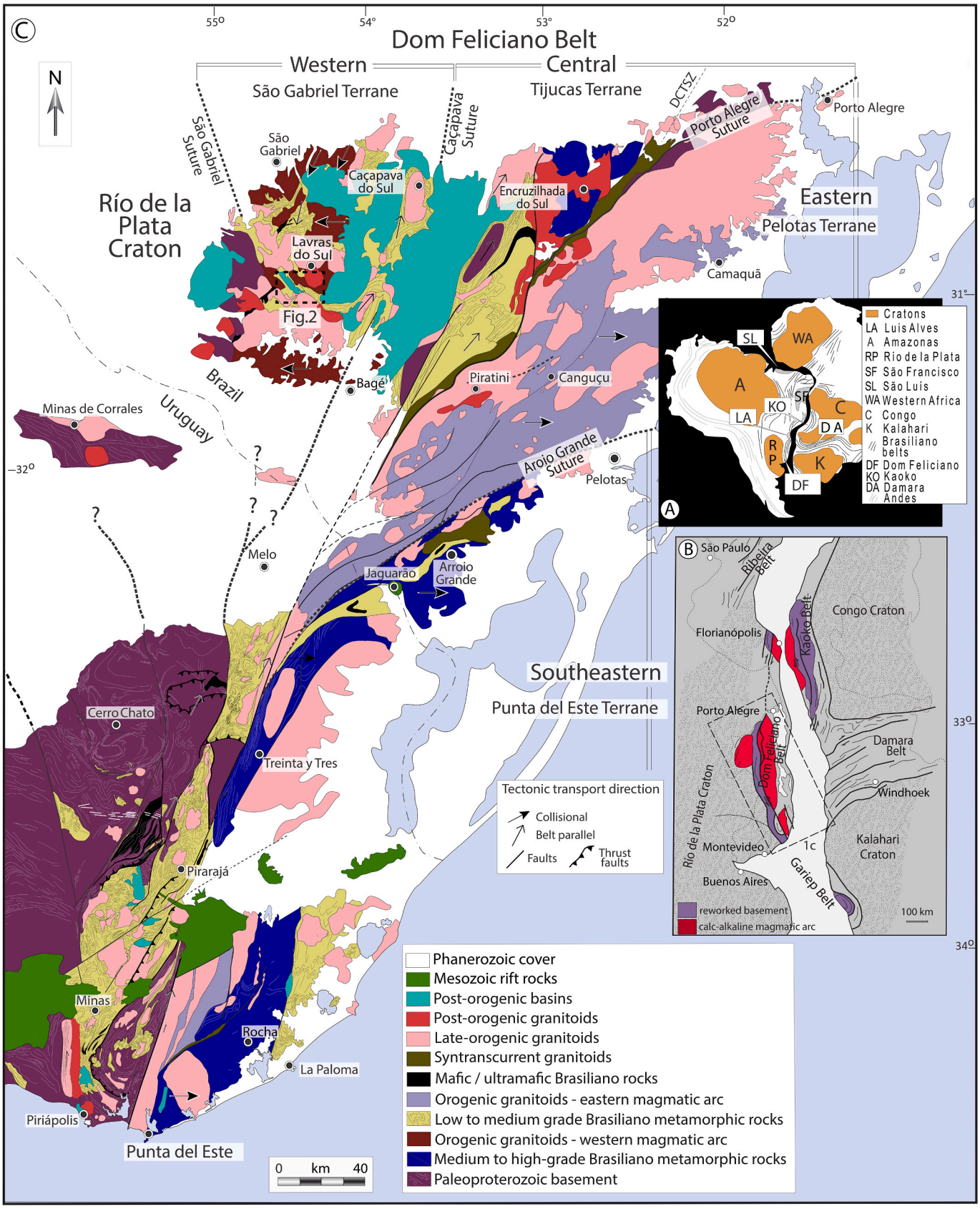

Fig. 1. Geological context of the Dom Feliciano Belt (modified from Masquelin et al., 2012; Ramos et al., 2018). A) Simplified map of the West Gondwana paleocontinent, showing the distribution of main cratons and mobile belts; B) Location of Dom Feliciano Belt and related African belts in the West Gondwana; C) Simplified geologic map of Dom Feliciano Belt and Río de la Plata Craton in southernmost Brazil (Rio Grande do Sul state) and easternmost Uruguay, showing the study area presented in Fig. 2 (black dashed square). DCTSZ = Dorsal de Canguçu Transcurrent Shear Zone.

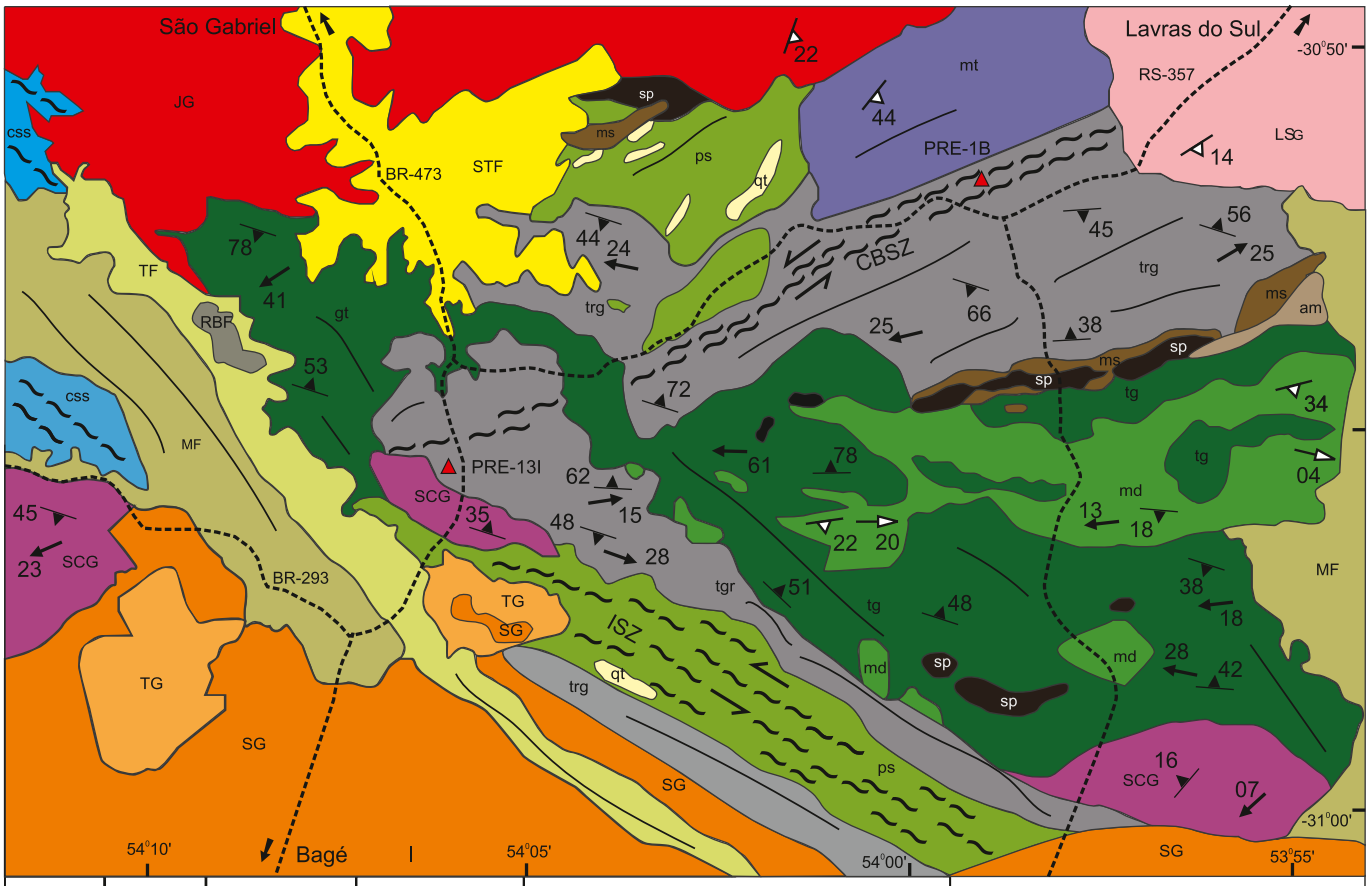

Era	Period	Unit	Legend	Main rock
Cenozoic	Paleogene 66 Ma	Santa Tecla Formation	STF	Conglomerate and sandstone
Paleozoic	Permian 299 Ma	Rio Bonito Formation	RBF	Sandstone and siltite
		Taciba Formation	TF	Conglomerate, sandstone and siltite (310 Ma)
Neoproterozoic	Ediacaran 635 Ma	Jaguari Granite	JG	Coarse equigranular monzogranite (570 Ma)
		Saibro Granite	SG	Coarse equigranular syeno and monzogranite
		Lavras do Sul Granite	LSG	Heterogranular syenogranite (598 Ma)
		Maricá Formation	MF	Conglomerate and sandstone
	Cryogenian 720 Ma	Tuna Granite	TG	Medium equigranular syenogranite
		Cambaí Complex	md / mt	Metadiorite and metatonalite (704-755 Ma)
	Tonian 1.0 Ga	Imbicuí Complex	tg / trg	Tonalitic and trondhjemitic gneiss (828-869 Ma)
		Sanga da Cachoeira Complex	SGC	Tonalitic gneiss
		Arroio Marmeleiro Complex	ps / qt / cs	Pelitic schist, quartzite and calc-silicate schist
		Cerro Mantiqueira Complex	ms / sp / am	Mg-schist, serpentinite and amphibolite (923 Ma)

Fig. 2. Simplified geological map of the Lavras do Sul region, São Gabriel Terrane, showing the main units. Red triangles are the location of outcrops with U–Pb samples dated. Modified from UFRGS (1991; 2004; 2005), Kraemer (1995), Laux (2017), and Philipp et al. (2018).

Laser-induced elemental fractionation and instrumental mass discrimination were corrected using the G91500 standard zircon. Uncertainties were calculated using error propagation. The ages were calculated using Isoplot software (Ludwig, 2003).

4. Results

4.1. Field aspects

The Imbicuí Complex comprises metatonalite and metatrondhjemite rocks and subordinately metadiorite, metaquartz diorite, and metagabbro. Dominantly outcropping in high strain zones, an mm-cm mafic and felsic irregular and discontinuous banding is characteristic. In low-strain

zones, the magmatic features are more pronounced with relicts of magmatic feldspars but always with granoblastic texture. The metagabbros, metadiorites, and metatonalites show interfingered contacts when in contact.

Metatrondhjemite is the dominant rock in the Imbicuí Complex. It is light grey, coarse-grained, and constituted by plagioclase, quartz, amphibole, and biotite (Fig. 3A). The outcrops of the studied metatrondhjemite occur surrounding the region of Cerro Branco, near the homonymous ductile, transcurrent shear zone (Siviero et al., 2022). The shear zone is about 10 km long, 700 m wide, E-W trending (Fig. 3B), and imprinting a heterogeneous deformation characterized by mylonitic domains in lithologies of the Imbicuí Complex. Igneous features such as feldspars porphyroclasts are preserved in a few areas where deformation is less intense.

The metadiorites and metaquartz diorites in the region are grey to green, fine-to medium-grained with granoblastic texture, and metamorphic foliation marked by mm bands of amphibole and plagioclase + quartz (Fig. 3C). The metatonalites are less abundant, pinkish, fine-to medium-grained, showing alternating felsic (quartz + plagioclase) and mafic bands (amphibole + biotite).

Locally, the Imbicuí Complex presents a coarse-grained metagabbroic rock with granoblastic texture (plagioclase + pyroxene), massive and crosscutting rocks from the Sanga da Cachoeira Complex (Fig. 3D).

Structural features that originated during amphibolite to greenschist facies deformation of the Lavras do Sul region rocks were divided into two broad groups: i) structures which are part of the main regional fabric and were formed during the ductile rock flow responsible for the accommodation of the principal deformation, and ii) the late structures, particularly open folds and ductile and brittle shear zones that affect and control the orientation of the older penetrative fabric. The main deformational fabric is a regionally expressed composite banding developed in high-strain zones. This foliation has been interpreted as being produced along a flat-lying shear zone responsible for the tectonic interleaving of the mafic-ultramafic sequence with deformed granitoids, as Imbicuí and Cambaí complexes (Siviero et al., 2022).

4.2. *Petrography*

The Imbicuí Complex presents an S = L fabric marked by the alternation of millimetric-centimetric mafic mineral slayers and felsic minerals bands, sometimes with millimetric biotite-aggregate boudins enveloping layers of quartz and feldspar defining an anastomosing metamorphic foliation and its gneissic aspect, which is registered by a main W-E sub-vertical metamorphic foliation (Fig. 4A). The rock foliation is arranged in granoblastic domains of quartz-feldspar with domains of white mica. Locally, metatrondhjemites present an L > S fabric characterized by mullions of quartz-feldspars aggregates (Siviero et al., 2022), which registers the main subhorizontal SE stretching lineation (Fig. 4B).

The quartz mylonite has a fabric S > L, where millimetric white mica bands are intercalated with quartz-feldspar bands. Layers of ribbon quartz, thin lamellae of mica, and fractured feldspar denote the mylonitic texture. Feldspathic quartz bands vary between 0.1 and 1 mm. Mica occurs as dark aggregates. The mica grains predominate as fish-like microstructure or polygonal. Secondary growth of chlorite occurs, forming an interlobated contact at the edge of the mica fish.

The Imbicuí Complex mineral assemblage consists of hornblende + plagioclase ± quartz ± biotite ± K-feldspar ± garnet ± oxide iron ± pyrite. The apatite, allanite, and zircon are the main accessory phases. The secondary mineral assemblage is composed of the muscovite ±

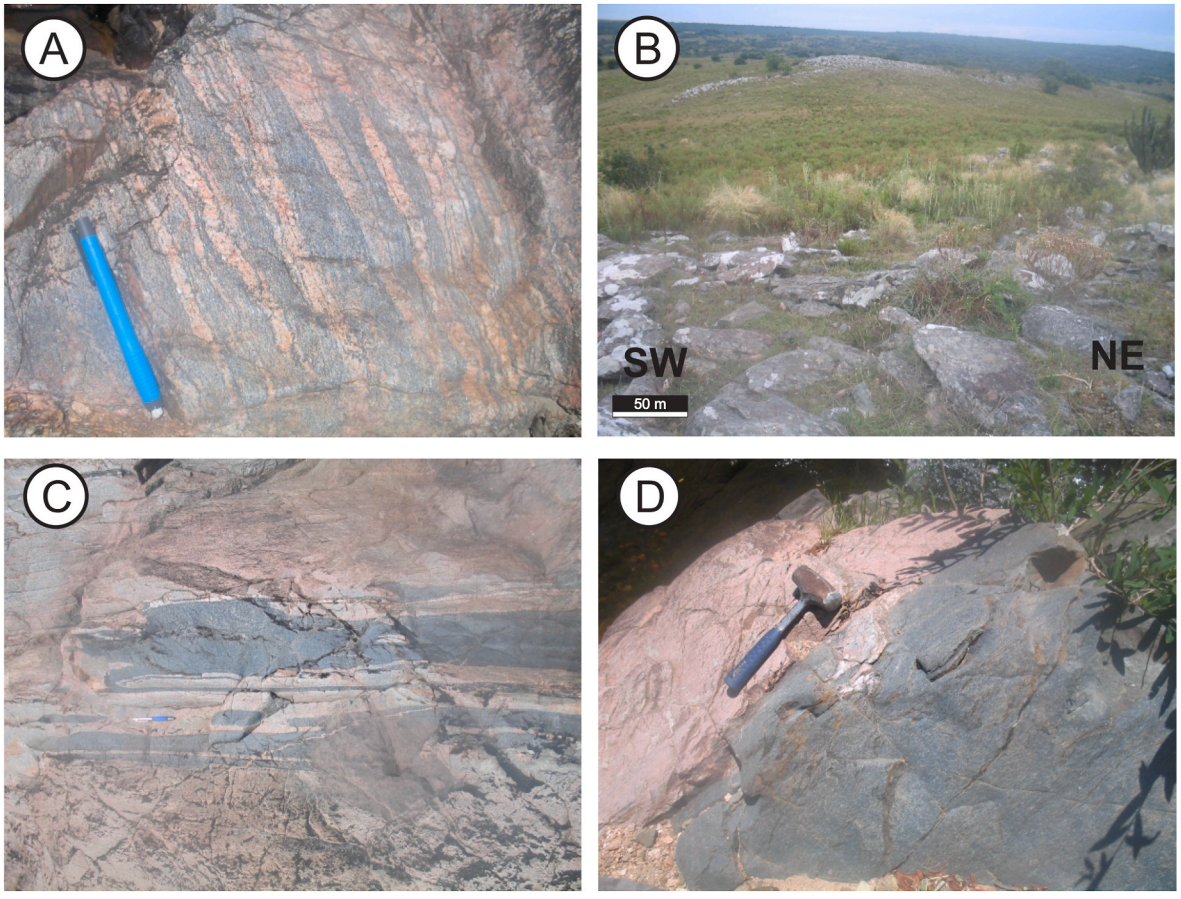

Fig. 3. Main outcrops of the Imbicuí Complex. A) Main textural aspects of metatrondhjemite (PRE-1B); B) Metatrondhjemite at Cerro Branco Shear Zone (PRE-1B); C) Quartz diorite banded showing sub-vertical metamorphic foliation. D) Metagabbroic rock (PRE-13I) crosscutting older unit (grey orange rock).

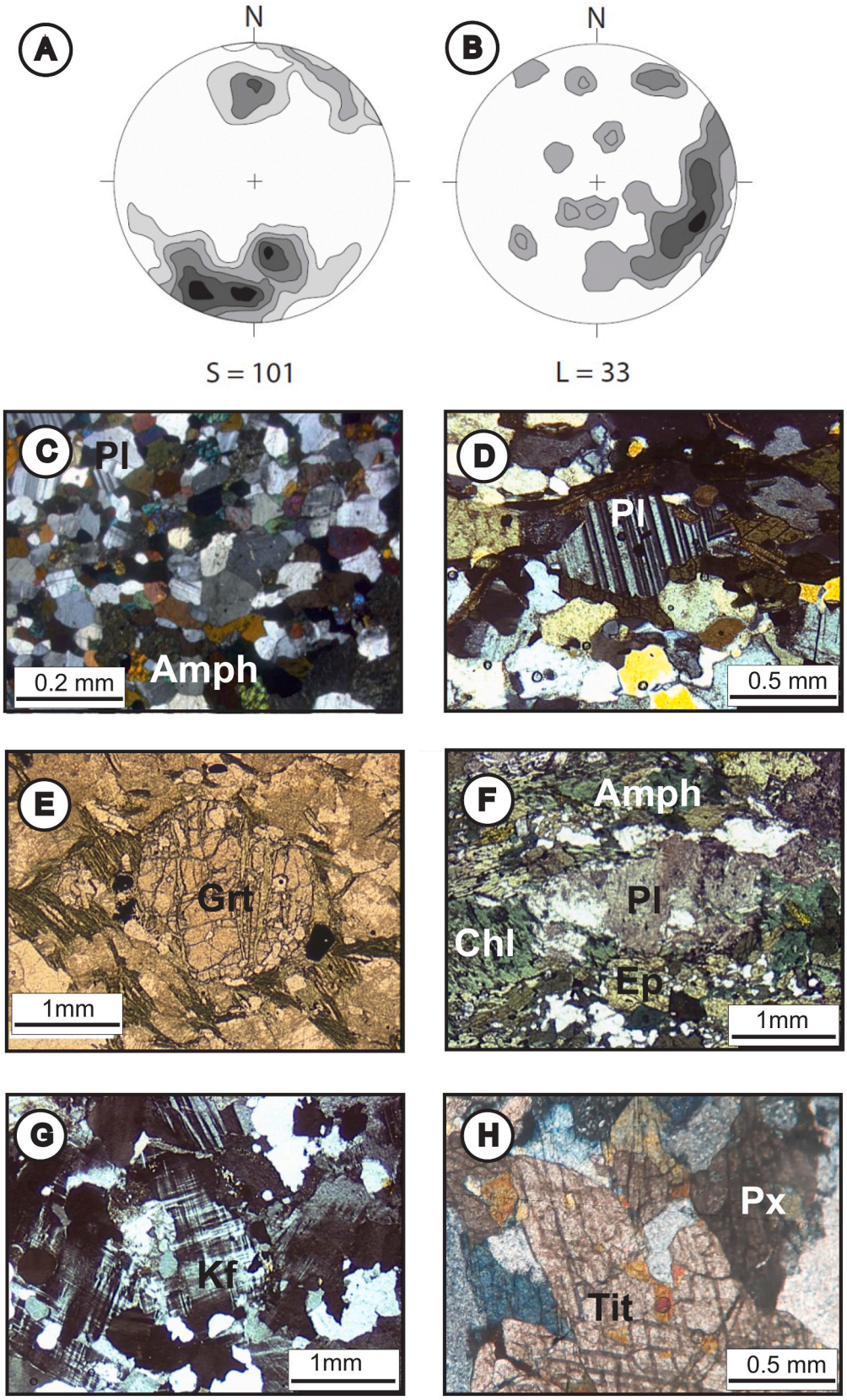

Fig. 4. Stereograms of S and L and photomicrography features of the Imbicuí Complex. A) The countoured stereogram (equal area lower hemisphere projection) of poles to metamorphic foliation planes; B) The countered stereogram (equal area lower hemisphere projection) of stretching mineral lineation; C) Granoblastic texture in metatonalitic rock; D) Plagioclase porphyroclast in metaquartz dioritic rock; E) Garnet porphyroblast in metatrondhjemitic rock; F) Plagioclase and amphibole with nematoblastic texture in metadioritic rock, and low-temperature retrogressive mineral assemblage composed of epitote, chlorite and saussuritic plagioclase; G) Quartz-alkali feldspars aggregate with ondulose extinction in metatonalite; H) Titanite and pyroxene in metagabbro (PRE-13I sample). Grt = garnet, Pl = plagioclase, Amp = amphibole, Kf = K-feldspar, Px = pyroxene, Chl = chlorite, Ep = epidote.

biotite ± sericite. Hornblende ± plagioclase recrystallization in granoblastic texture suggests an amphibolite facies metamorphism to the Imbicuí Complex rocks (Fig. 4C).

Plagioclase occurs as granoblastic grains with wavy extinction and size of 0.2–0.5 mm, forming equidimensional grain aggregates with quartz and K-feldspar, the formers always with < 0.1 mm, in aggregates in the matrix. Locally porphyroclasts of plagioclase occur with a size of 0.5 cm, subhedral, long and short rectangles, polysynthetic twinned, and the composition is andesine (Fig. 4D). The photo-micrograph shows a quartz-feldspathic rock comprising equidimensional quartz, plagioclase, biotite, and amphibole crystals. Some contacts are lobate-cuspate. All the plagioclases show the characteristic albite twins. Some contacts between feldspar grains indicate grain-boundary migration recrystallization and some grain boundary area reduction (triple points).

Garnet is a common mineral in metatrondhjemites, in general euhedral, with 0.5 mm, as porphyroblast (Fig. 4E). Amphibole is the mafic phase predominating with anhedral to subhedral sizes between 0.5 and 1.5 mm, also occurring as granoblastic aggregates, locally with 0.4 mm, and a nematoblastic texture (Fig. 4F).

Quartz generally occurs as anhedral grains with a variable size of up to 4.0 mm; straight contacts, a wavy extinction, and chessboard patterns are present. In some diorites, quartz commonly occurs in a particular globular form with a 0.1 mm diameter in alkali-feldspar and amphiboles (Fig. 4G).

Biotite occurs with pleochroism varying from green to brown-reddish and sizes of 0.3–2.5 mm, forming aggregates surrounding amphibole. The contacts are straight with these minerals and sometimes show chlorite substitution and/or the presence of mm chlorite aggregates.

Euhedral iron oxide grains occur disseminated in a quartz granoblastic and plagioclase matrix. The pyrite, in general, is euhedral cubes, reaching up to 1 mm, happening disseminated, mainly in basic terms. The zircon and apatite phases are widely spread into intermediaries to acidic lithotypes, generally euhedral and up to 0.5 mm.

The metagabbro rocks present distinctive petrographic aspects in the Imbicuí Complex, mainly registered by the extensive presence of titanite crystals and the absence of garnet compared to other rocks in the complex. The plagioclase + titanite + pyroxene ± epidote represents the metamorphic mineral assemblage, always with granoblastic texture, suggesting an amphibolite facies metamorphism for these rocks (Fig. 4H).

Titanite varies from 0.3 to 0.5 mm and has a brown color, with dominant anhedral shapes, but also occurs as inclusions in other minerals, such as epidote. Plagioclase (0.5–1.2 mm) is euhedral, with polygonal texture and intense sericitization. Epidote (0.05–0.5 mm) occurs as rounded inclusions or partially replacing the titanite and plagioclase. Pyroxenes (0.3–0.7 mm) are subhedral, scattered in the sample, and occur as aggregates. Zircon, apatite, and magnetite occur as an accessory phase. Chlorite and carbonate represent secondary minerals.

4.3. Whole-rock geochemistry

The Imbicuí Complex whole-rock geochemistry results are summarized in Supplementary Table 1. These geochemical data were used to characterize the magmatic processes, sources, and tectonic environment of the rocks of the Imbicuí Complex and to study the elements' mobility. The mobile element data and whole-rock geochemistry analyses were compared with the igneous trend presented in the MFW diagram (Ohta and Arai, 2007), where samples plotted near this igneous trend, precluding minor alteration and/or metamorphism element mobility in the bulk composition rocks of this complex.

The complex comprises rocks with high-SiO_2 (63.90–72.14 wt%), Al_2O_3 (14.48–19.55 wt%), and alkalis (4.69–8.09 wt%) contents, with Na_2O (3.67–7.03 wt%) concentrations higher than K_2O (0.33–3.05 wt %). The Imbicuí Complex is also relatively enriched in CaO (1.3–4.64 wt %) and Fe_2O_3 (1.13–3.23 wt%), concerning MgO (0.17–1.68 wt%). TiO_2 and P_2O_5 occur only as low trace amounts.

Regarding the classification using the TAS diagram (Middelmost, 1994), normative of all rocks of Imbicuí Complex spread over the granodiorite-granite fields, showing a sub-alkaline character (Fig. 5A). A dominant calc-alkaline pattern is observed for Imbicuí Complex rocks, with exception to sample PRE-13I, with a tholeiitic affinity in AFM diagram (Fig. 5B). In the K–Na–Ca diagram (Fig. 5C) from Barker (1979), a trondhjemitic trend (or low calc-alkaline trend) is observed to Imbicuí Complex rocks, also plotting in the adakitic field. In the Shand (1943) diagram (Fig. 5D), the samples plot mainly in the metaluminous to the peraluminous field (A/CNK < 1.2, represented by the vertical dashed line in the diagram), showing a subhorizontal trend. In the Harker diagrams for major and trace elements is observed a negative correlation regarding the Al_2O_3, Fe_2O_3, MgO, MnO, TiO_2, P_2O_5, Rb, Sr, and Ba, a scattered correlation in the K_2O, Na_2O, Ba and Y diagrams.

The Sr contents are 573.5–1337 ppm for SiO_2 > 69.23 wt%. However, in a sample, the content of Sr is above 1558 ppm for SiO_2 = 65.72 wt%. The Y contents are 4.8–15 ppm resulting in Sr/Y between 67.2 and 169.92. For samples with SiO_2 = 65.72 wt% corresponding Y content 24 ppm (Sr/Y = 64.08). Adakites are characterized by high LILE, particularly Sr and low Y. Using the proposed classification of Barker (1979), Martin (1986), Drummond and Defant (1990), and Defant and Kepezhinskas (2001), which separates trondhjemite and tonalite in groups for the content of SiO_2 and Al_2O_3, all rocks with SiO_2 content 70 wt% and Al_2O_3 content greater than 15 wt% and according to these authors are called High-Al_2O_3 trondhjemites. A high-silica and low-silica adakites (HSA-LSA) is a classification based on Sr-(SiO_2/MgO)*100-K/Rb triangular diagram (Defant and Kepezhinskas, 2001) and the Imbicuí Complex is classified as high silica adakites-like rocks (Fig. 6A, B, C).

In the multi-element spidergrams, rocks from Imbicuí Complex show similar general patterns, commonly enriched in LILE elements (Rb) and lightly depleted in HFSE (Dy, Y, Yb, and Lu), with anomalies of P, Ti, and Nb.

The Imbicuí Complex rocks show regular distribution with slight enrichment in LREE, low to moderately fractionated patterns (La_N/Yb_N = 1.0–24.7), Eu anomalies (Eu/Eu* = 0.8–1.2), and ΣREE from 20.8 to 152.1 ppm. The REE patterns (Fig. 7) show evident enrichment compared to the chondrite model (Sun and McDonough, 1989). One sample presents a distinct pattern (PRE-13I) with a flat horizontal shape, similar to mantle primitive but ten times higher.

4.4. U–Pb geochronology

To estimate the crystallization age of the studied rocks, U–Pb (LA-MC-ICP-MS) analyses were performed in zircon crystals from samples PRE-1B and PRE-13I (Supplementary Table 2). The analyzed zircon grains are subhedral to anhedral. Their length and width proportion varies between 2:1 and 1:1 (predominance of 2:1), and grain size between 100 and 200 μm (Figs. 8 and 9). Some zircon grains show internal oscillatory zoning in the crystals is interpreted as primary, formed during igneous crystallization (Corfu et al., 2003).

The obtained U–Pb LA-MC-ICP-MS data are given in Supplementary Table 2 and plotted on Concordia diagrams (Fig. 10A and B). The diagram of the sample PRE-1B shows a Concordia age of 828 ± 8 Ma, which is interpreted as the igneous crystallization age of the protolith. The sample PRE-13I shows a Concordia age of 845 ± 3 Ma, interpreted as the protolith's igneous crystallization age, and the zircon crystals with ages between 920 and 950 Ma (Supplementary Table 2) are interpreted as inherited.

4.5. Whole-rock Sr-Nd-Pb isotope geochemistry

Two samples from the Imbicuí Complex were analyzed for Rb–Sr, Sm–Nd, and Pb–Pb (Supplementary Table 3). The isotopic values of the $^{87}Sr/^{86}Sr_{(828)}$ ratio ranged from 0.703473 to 0.707205. The isotopic

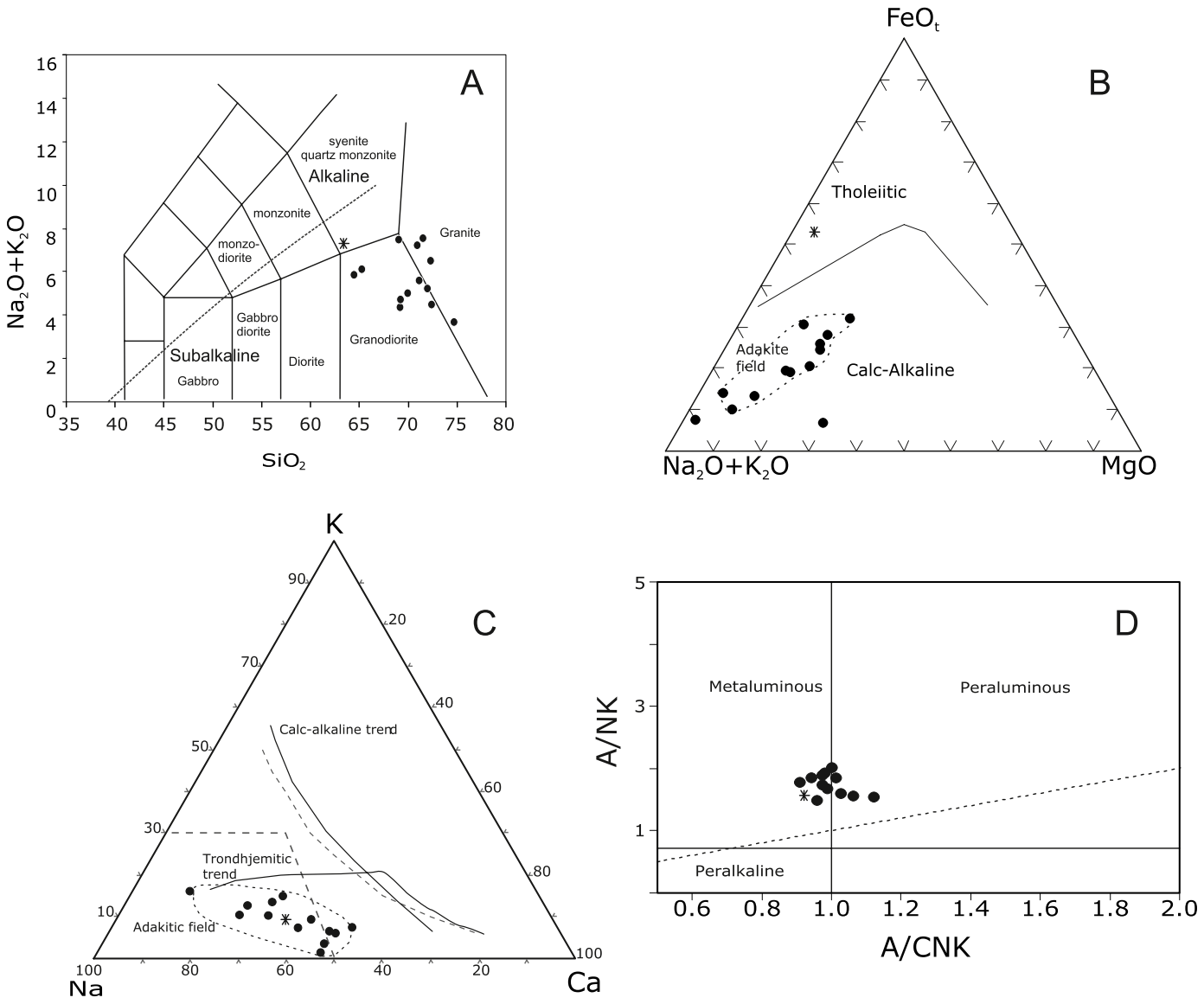

Fig. 5. Geochemical diagrams for Imbicuí Complex rocks. A) TAS diagram (Middelmost, 1994). The dashed line separates the field of alkaline and sub-alkaline affinity. B) AFM diagram, the black line separates the tholeiitic and calc-alkaline fields. Adakite field (dashed line) from Barker (1979). C) K–Na–Ca diagram from Barker (1979) shows the calc-alkaline trend (black line and dashed line) and the trondhjemitic trend. Adakitic fields are displayed, modified from Drumont and Defant (1990). D) Molar A/CNK ($Al_2O_3/CaO + Na_2O + K_2O$) vs A/NK ($Al_2O_3/Na_2O + K_2O$) diagram (Maniar and Piccoli, 1989) with the dominance of weakly peraluminous rocks in the Imbicuí Complex. Circles represent the main metatrondhjemites and tonalites specimens in the study area, while asterisk is a subordinate metagabbro type (sample PRE-13I).

values of the $^{143}Nd/^{144}Nd_{(828)}$ ratio ranged from 0.511991 to 0.511952, while $\varepsilon Nd_{(828)}$ values range from 8.2 to 7.5, and the Nd-T_{DM} model age range from 0.8 to 0.9 Ga. The isotopic values of the $^{207}Pb/^{204}Pb$ and $^{206}Pb/^{204}Pb$ ratio for the Imbicuí Complex ranged from 15.4908 to 15.5589 and 17.7054 to 18.4040, respectively.

5. Discussion

5.1. Geochemistry of adakites in the São Gabriel Terrane

The dioritic-tonalitic-trondhjemitic rocks of the Imbicuí Complex can be classified as adakite-like following the classification of Defant and Dumond (1990), as they have intermediate to high SiO_2 (> 63%), high Sr/Y (~100) and La/Yb (~25), with calc-alkaline affinity. The Yb content for these complex rocks is generally low (< 3.5 ppm), while the La/Yb ratios are less than 36.29, K_2O/Na_2O ratios < 0.71, usually similar to adakites (respectively, > 0.5; average 20.4; average 0.42) according to the classification of adakites by Martin (1999).

From the classification of high or low SiO_2 (Martin et al., 2005; Zhang et al., 2019), the adakites of the Imbicuí Complex can be classified as of the high SiO_2 type, with values, in general, higher than 63%, having as the dominant source melting of ocean plate rocks (cf. Moyen, 2009).

The Imbicuí Complex has a range of Al_2O_3 from 14.48 to 18.18 and high levels of SiO_2 and K_2O similar to Type 1 adakites from Lebedev et al. (2019). The molar Mg# of Type 1 adakites, in general, are higher, equivalent to 55, due to the melting of MORB type rocks and the interaction of this magma with the mantle wedge, whereas Type 2 adakites have lower values, less than 45, without interaction with peridotites during their ascent. The adakites of the Imbicuí Complex show low Mg# values (< 43.97), suggesting little interaction with the peridotitic mantle's wedge.

In the Imbicuí Complex, the rocks are rich in Sr (573.5–1538 ppm), poor in Y (< 35.5 ppm), and are positioned in the field of adakites and

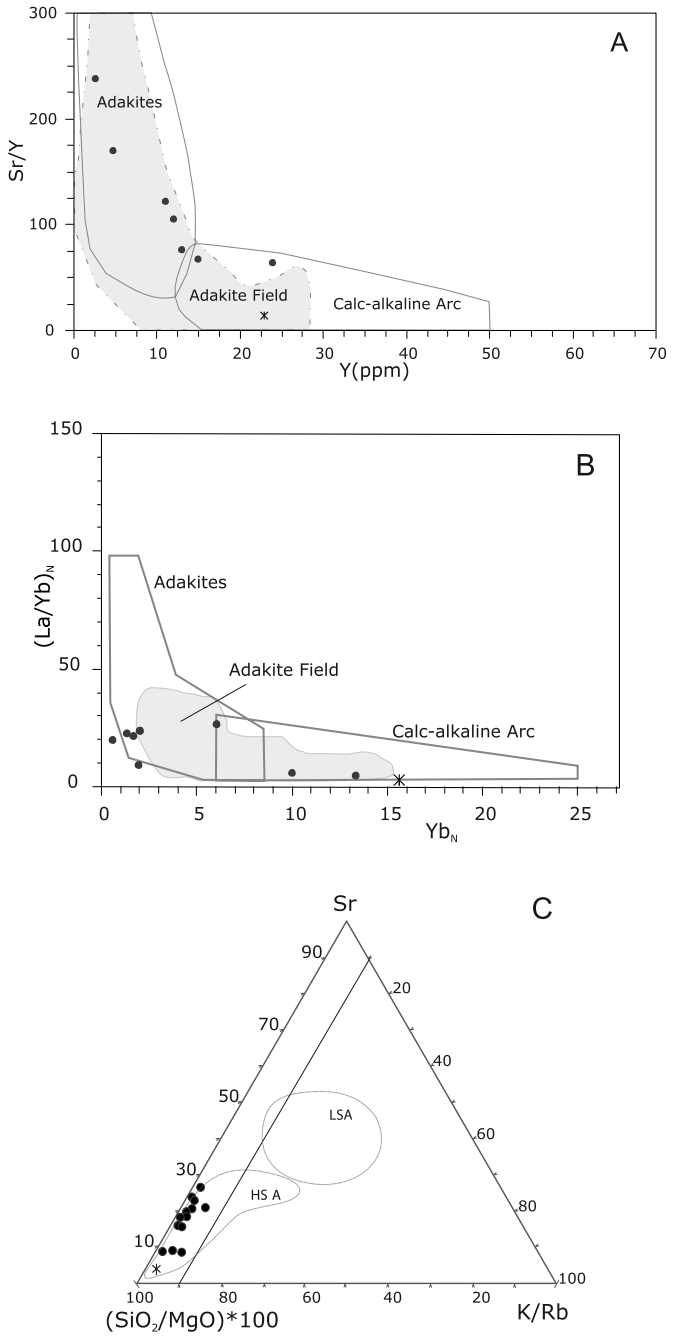

Fig. 6. Discrimination diagrams for Imbicuí Complexá rocks. A) Sr/Y vs Y diagram discrimination of adakites and calc-alkaline arc rocks and also the adakite field (grey field), modified from Drummond and Defant (1990); B) Chondrite-normalized $(La/Yb)_N$ vs Yb_N diagram discrimination of adakites and calc-alkaline arc rocks and also the adakite field (grey field), modified from Martin (1986); C) Sr-(SiO_2/MgO)*100-K/Rb triangular diagram from Defant and Kepezhinskas (2001). LSA = low-SiO_2 adakite and HSA = high-SiO_2 adakite. Symbols as in Fig. 5.

TTG in the Sr/Y vs Y diagram (Fig. 6A). In the Sr/Y vs Y or $(La/Yb)_N$ vs Yb_N diagram, the chemical composition of the rocks of the Imbicuí Complex plot in the adakite and TTG fields and the andesite, dacite and arc rhyolite fields (Defant et al., 1992).

A tholeiitic affinity is observed in metagabbros (sample PRE-13I) from the Imbicuí Complex, which has the highest Al_2O_3 content (19.55 ppm) and distinct Sr (323.3 ppm) and Y (22.9 ppm) values when compared to the main Imbicuí Complex rocks.

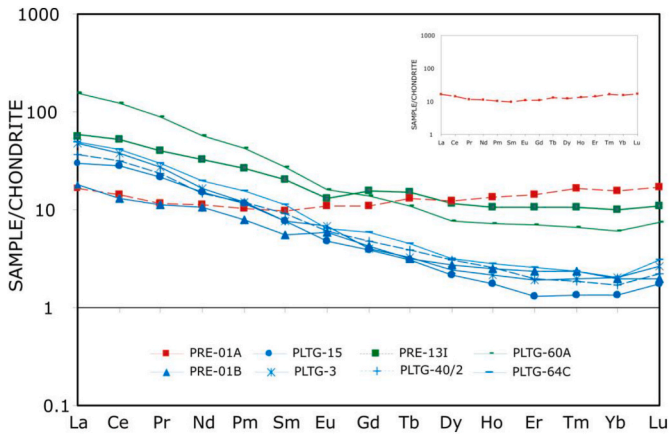

Fig. 7. REE chondrite diagram normalized (Sun and McDonough, 1989) of the Imbicuí Complex rocks. Detailed sample PRE-13I, with a flat pattern and different Eu anomalies.

5.2. Sr-Nd-Pb isotopes in adakites from São Gabriel Terrane

The Imbicuí Complex rocks were compared isotopically with ortho-derivated rocks of the Cambaí Complex (Saalmann et al., 2005a, 2005b; Siviero et al., 2021), and the ultramafic rocks (serpentinites) and amphibolites of the Cerro Mantiqueira Complex (Leite et al., 1998).

The rocks of the Imbicuí Complex present high positive values of $\varepsilon Nd_{(828)}$, as shown in the $\varepsilon Nd_{(0)}$ vs age diagram (Fig. 11A). The Nd-T_{DM} vary between 0.8 and 0.9 Ga, similar to this unit's crystallisation ages. An age of 828 Ma is proposed in this work, whereas 879 Ma has been presented by Leite et al. (1998). When comparing the rocks of the Cerro Mantiqueira Complex, the evolution lines are similar, with variations of $\varepsilon Nd_{(828)}$ and Nd-T_{DM}, respectively, from −3 to 2 and 0.8 to 1.2 Ga. Compared with the rocks of the Cambaí Complex, they present a similar Nd isotopic behaviour. The source of the magmatism of the Imbicuí Complex can also be discussed in the Sr–Nd diagram calculated at 740 Ma (to compare with Cambaí Complex, which presents similar U–Pb crystallization age), shown in Fig. 11B, as well as being compared with the rocks Cerro Mantiqueira and Cambaí complexes.

It should be noted that the mantle end-members used (PM, DM, EM-I, EM-II, HIMU, Zindler and Hart, 1986; Rollinson, 1993) was used as a comparison of similar modern analogues since the Neoproterozoic mantle cannot reflect the composition of these current reservoirs (Blichert-Toft et al., 2010). The mantle end-members are the primitive mantle (PM), the depleted mantle (DM) and the enriched mantles (EM-I and EM-II), and U and Pb enriched mantles due to the recycling of basaltic ocean crust (High-μ) as discussed in Faure and Mensing (2005), Condie (2005); Gill (2010) among others. About these reservoirs, as well as the rocks of the Cerro Mantiqueira Complex, the Imbicuí Complex rocks have an $\varepsilon Nd_{(740)}$ behaviour similar to the depleted mantle (DM) and primitive mantle (PM) but with $^{87}Sr/^{86}Sr_{(740)}$ ratios more enriched to these. When comparing the Cambaí Complex rocks, the Imbicuí Complex shows similar behaviour. Thus, a suitable scenario for the generation of the rocks of the Imbicuí Complex may be the melting of rocks with isotopic compositions similar to that of the Cerro Mantiqueira Complex, that is, the melt of a mantle member, similar to amphibolites or PM (primitive mantle) or DM (depleted mantle) end-members.

The diagram in Fig. 11B was conceived for current rocks, and the plot of Tonian rocks is speculative, especially with few samples. The isotopic Sr initial ratio of the only two samples is different, denoting heterogeneity in the Sr system. Sample PRE-1B shows an $^{87}Sr/^{86}Sr_{(828)}$ of 0.704143 representing the primitive Sr isotopic signature, while secondary processes modified sample PRE-15 B (e.g., saussuritic plagioclase), and thus this sample must be carefully used in interpretations.

In diagram $^{207}Pb/^{204}Pb$ vs $^{206}Pb/^{204}Pb$ (Fig. 11C), the behaviour of

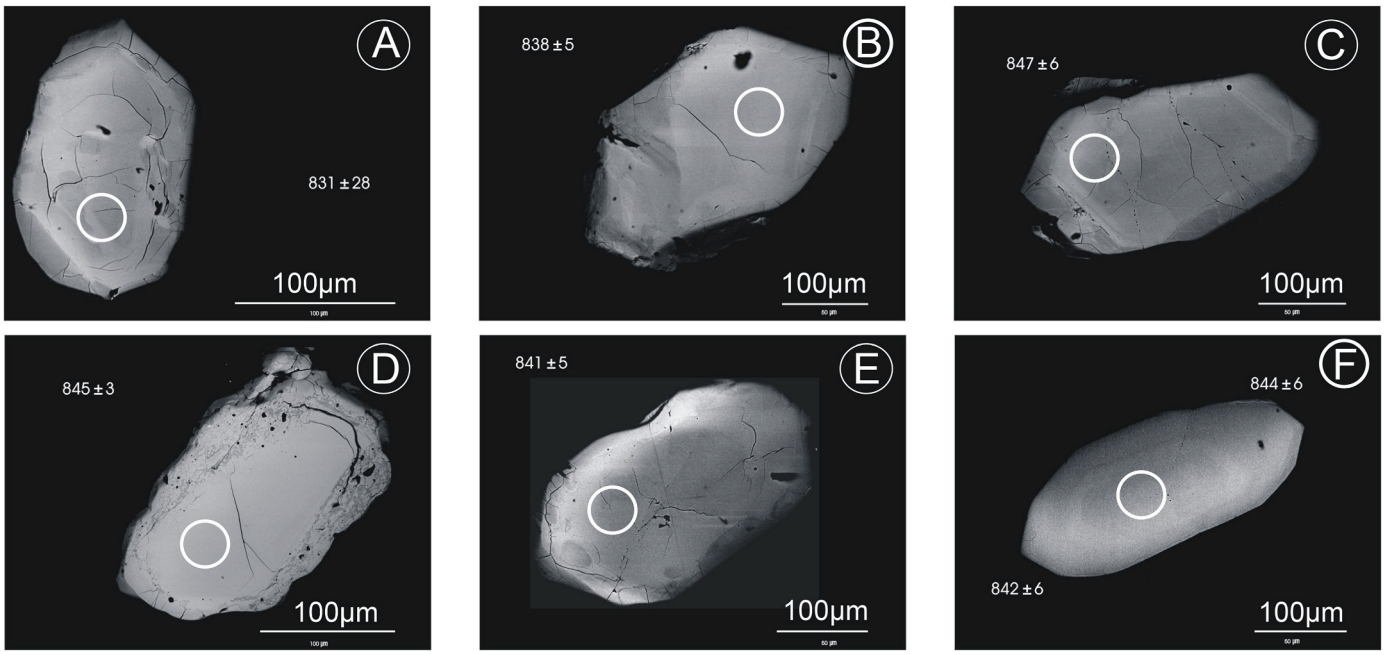

Fig. 8. Cathodoluminescence images of Imbicuí Complex's zircons (PRE-1B). A) Euhedral zircon crystal, with metamict zonation and opaque mineral inclusions. B, C, D) Euhedral zircon showing magmatic zonation in the core to rim. E, F) Euhedral zircon showing magmatic zonation in the core.

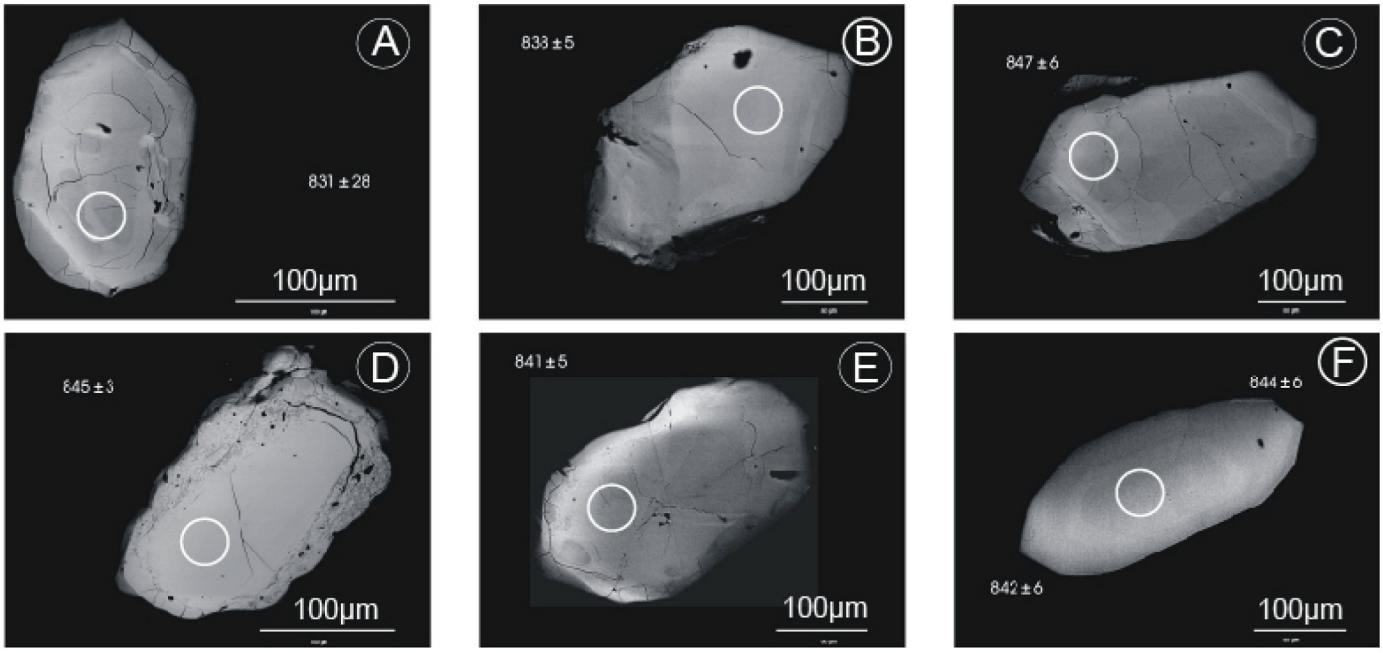

Fig. 9. Cathodoluminescence images of zircons of the Imbicuí Complex (PRE-13I). A,B) Euhedral zircon crystal, with fair zonation. C,D,E,F) Subhedral zircon showing a fair zonation in the core and a metamict rim.

the rocks of the Imbicuí Complex is compared to the mantle end-members (PM, HIMU, DM, EM-I, EM-II) and the rocks of the Cerro Mantiqueira Complex and Cambaí Complex. Samples from the Imbicuí Complex plot above the mantle evolution curve and close to the orogen evolution curve. These rocks have isotopic compositions similar to those of the Cerro Mantiqueira Complex and the Cambaí Complex. A mantle source of the HIMU type (High-μ), a signature of rocks generated from recycled ocean plates ($^{206}Pb/^{204}Pb > 21.5$; Weiss et al., 2016), can be discarded due to isotopic $^{206}Pb/^{204}Pb$ analyses lower than 19 to the Imbicuí Complex rocks.

The Sr-Nd-Pb isotopic compositions of the Imbicuí Complex reveal an $^{87}Sr/^{86}Sr_{(i)}$ ratio of 0.704143 for the metatrondhjemite rock of the complex's PRE-1B sample and 0.709107 for the PRE-15 A sample. The increased Sr isotope content can be attributed to various geological processes (Gill, 2010). Among the key contributors to strontium enrichment in rocks are: (i) subduction of sediments, (ii) fluid-rock interaction, (iii) enriched mantle melting, (iv) sedimentary contamination, and/or (v) metasomatic-secondary alterations. The elevated strontium content observed in the Imbicuí Complex rocks (e.g., 0.709107 for the PRE-15 A sample) may arise from one or more processes. On the other hand, the 0.704143 ratio for the metatrondhjemite rock (PRE-1B sample) reflects a more representative sample, possibly

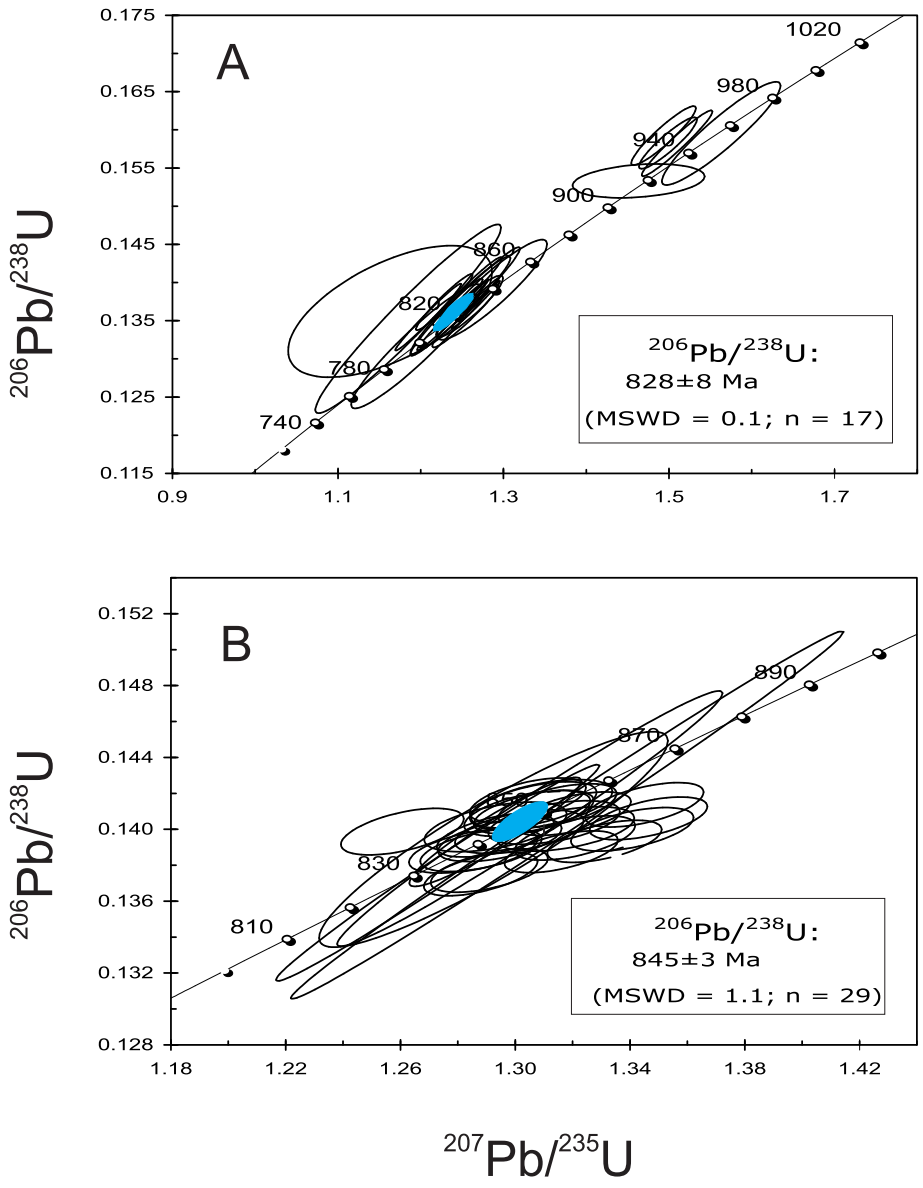

Fig. 10. U–Pb LA-ICP-MS zircon geochronology in the Imbicuí Complex. A) Concordia diagram of metatrondhjemite (PRE-1B) with a crystallization age of 828 ± 8 Ma. B) Concordia diagram of metagabbro (PRE-13I) with a crystallization age of 845 ± 3 Ma.

less influenced by metasomatic-secondary alterations or indicative of a geological process such as crustal contamination. As the lead isotopes are less mobile compared to Sr, they are anticipated to be minimally impacted by metasomatic-secondary alterations.

The $^{143}Nd/^{144}Nd_{(828)}$ values ranging from 0.511991 to 0.511952 suggest an Nd-isotopic homogeneous source. This interpretation of a single and homogeneous source for the generation of adakites. Isotopic Sr could be interpreted as i) Sr mobility by post-magmatic processes or ii) Sr-isotopically enriched material contamination, such as, for example, sediments from oceanic slab melting.

5.3. Source of adakites in the São Gabriel Terrane

Recent works by adakites in the world postulate a genesis from melting a slab from the oceanic plate. The term "slab" is broader, not only representing the portion of "basaltic" rocks but also with the contribution of sediments to explain Sr isotopic enriched signatures, such as, for example, Gomez-Tuena et al. (2003) for North American adakite rocks. Anomalies of Nb and Ta are common, and the variation of incompatible elements such as Rb and Ba may be due to the incorporation of sediments during slab melting, which can also affect the isotopic compositions of adakites (e.g., Bebout et al., 1999). In NW China, adakites (375 Ma) described by Zhang et al. (2005) have $^{87}Sr/^{86}Sr$ isotopic ratios of 0.70466–0.70490 and εNd between 3.02 and 4.06, slightly different from typical MORB values (0.70365 and εNd > 5.1; Pyle et al., 1992) and suggest that sediments were incorporated into adakites during the slab melting.

Amphibolite, eclogite, and garnet amphibolite melting curves, a petrological model for adakites suggested by Rapp et al. (1999), improved by Takahashi et al. (2005) and Zhang et al. (2019) suggest altered MORB as the main source of these rocks. In the $(La/Yb)_N$ vs Yb_N diagram (Fig. 12), the rocks of the Imbicuí Complex present a behaviour similar to those formed by the melting of eclogites or a high amount (25%) of garnet amphibolite, suggesting these adakites can be formed from by slab melting of an oceanic crust similar to MORB. The evolved chemical composition of the rocks in the complex favours this hypothesis since, in general, these rocks have SiO_2 contents > 65%.

The metagabbro rocks from Imbicuí (sample PRE-13I) present a SiO_2 content of 63%, but as suggested in the $(La/Yb)_N$ vs Yb_N diagram (Fig. 12), a distinct source can be envisaged for it, with amphibolites as the main source.

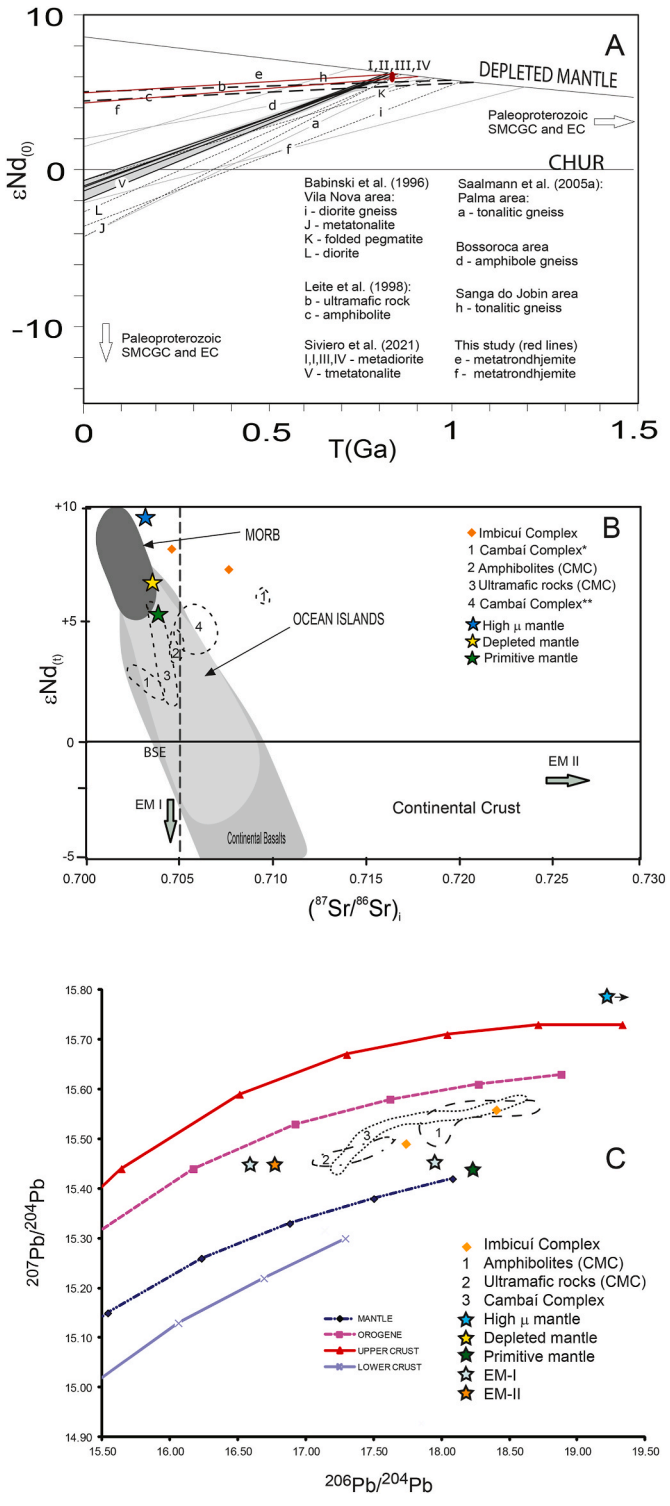

Fig. 11. Isotopic diagrams for the Imbicuí Complex. A) Diagram $\varepsilon Nd_{(0)}$ vs time of the Imbicuí Complex (modified from DePaolo, 1981) compared with other rocks from the literature in the São Gabriel Terrane. DM = Depleted mantle, CHUR = chondritic uniform reservoir. Red lines are metatrondhjemite from this study. SMCGC = Santa Maria Chico Granulitic Complex; EC = Encantadas Complex; red ellipse represents the crystallization age of the Imbicuí Complex (828 Ma). B) Diagram $\varepsilon Nd_{(t)}$ vs $^{87}Sr/^{86}Sr_{(i)}$ for the (modified from DePaolo, 1981) mantle end-members (calculated for 740 Ma) were extracted from Zindler and Hart (1986) and Rollinson (1993). HIMU (mantle with high U–Pb ratio), DM (depleted mantle), PM (primitive mantle); EM-I (enriched mantle I), EM-II (enriched mantle II). 1 - Cambaí Complex* = data from Saalmann et al. (2005a,2005b); 4 – Cambaí Complex** = data from Siviero et al. (2021); CMC = Cerro Mantiqueira Complex from Leite et al. (1998). C) Diagram $^{207}Pb/^{204}Pb$ vs $^{206}Pb/^{204}Pb$ for the Imbicuí Complex in comparison with the mantle end members (Zindler and Hart, 1986; Rollinson, 1993; HIMU (mantle with high U–Pb ratio), DM (depleted mantle), PM (primitive mantle); EM-I (enriched mantle I), EM-II (enriched mantle II)) and others rocks from the literature in the São Gabriel Terrane. CMC = Cerro Mantiqueira Complex from Leite et al. (1998); Cambaí Complex data from Siviero et al. (2021).

(caption on next column)

The fractional crystallization of primitive magmas derived from mantle wedge melting has also been postulated to generate adakites (Takahashi et al., 2005). However, the fractional crystallization curve of adakitic magmas with the crystallization of hornblende + biotite + plagioclase shows that the rocks of the Imbicuí Complex are not close together, suggesting that this process was not the most effective. The rocks generated by melting fluid-rich wedge mantle peridotite generally have high K_2O values, positioning the rocks in the medium to high-K calc-alkaline field. Still, the rocks of the Imbicuí Complex also show low K_2O ratios, an overall < 3.05 (mean 1.06), defining these rocks with the trondhjemitic character (or low-K calc-alkaline).

Thus, for the Imbicuí Complex adakites, the high SiO_2, Al_2O_3, and Na_2O content and low MgO content suggest that the melting of eclogitic rocks has been effective. Besides, the content of Y and HREE, especially Yb, can mean partial melting of a hydrated basalt or amphibolite garnet under specific conditions of pressure and temperature (2.5 kbar, 850 °C), as the garnet is stable in these conditions. At the same time, plagioclase is not stable, with depletion in Y and Yb attributed to the fact that the garnet remains in the residue, retaining them (Naqvi and Prathap, 2007). High values of Sr suggest the absence of plagioclase in the residue, while low values of Y and Yb, high Sr/Y, and La/Yb indicate garnet, clinopyroxene, and hornblende in the source (Defant and Drummond, 1990).

The Imbicuí Complex presents low levels of Nb, on average 12 ppm, and therefore cannot be called Nb-enriched basalts (Defant et al., 1992) or high-Mg adakites (HMA, Zhang et al., 2019) generally associated with slab delamination and asthenospheric sources. Sources generated from the melting of either the lower mafic crust or underplated mafic magmas often produce low SiO_2 adakites (Castillo, 2012; Ribeiro et al., 2016), while continental adakites (Moyen, 2009) or C-type adakites (Zhang et al., 2019) have high K_2O/Na_2O ratios, incompatible with those of the Imbicuí Complex, which present low K_2O/Na_2O ratios values.

In the Imbicuí Complex, an isotopic comparison with Cambaí Complex's rocks, a magmatic arc of 750–700 Ma in the São Gabriel Terrane (Saalmann et al., 2005a, 2005b; Siviero et al., 2021) and mafic-ultramafic rocks (amphibolites and serpentinites) of the Cerro Mantiqueira Complex (Leite et al., 1998), which represent an oceanic plate obducted in the region (923-733 Ma, Leite et al., 1998; Arena et al., 2016), matches the same material in their sources.

In the $\varepsilon Nd_{(o)}$ vs age diagram (Fig. 11A), the study rocks in the Imbicuí Complex show positive $\varepsilon Nd_{(o)}$ and $\varepsilon Nd_{(828)}$ values, similar to those of the mafic-ultramafic rocks. However, the rocks of the Cambaí Complex have $\varepsilon Nd_{(0)}$ negative and $\varepsilon Nd_{(740)}$ positive. The samples of the Imbicuí Complex have model Nd-T_{DM} ages (0.8–0.9 Ga), similar to the crystallization age of the complex (828 Ma, PRE-1B), the Cambaí Complex has model Nd-T_{DM} ages (0.7–1.0 Ga) close by its crystallization ages of 740 Ma (Leite et al., 1998; Siviero et al., 2021), as well as the mafic rocks of the Cerro Mantiqueira Complex with ages model Nd-T_{DM} (0.7–1.2 Ga) suggesting that the original magmas are juvenile.

Strontium and Nd isotopes show signatures similar to those of the meso-oceanic ridge basalts (MORB) trend, as observed by Kimura et al. (2014) in Japan and also suggested by Defant et al. (2012) for French adakites. In the Imbicuí Complex, the isotopic values of Sr and Nd show a similar trend to that of MORB-Ocean Island for 740 Ma. The complex data were also compared with mafic-ultramafic rocks (amphibolites and

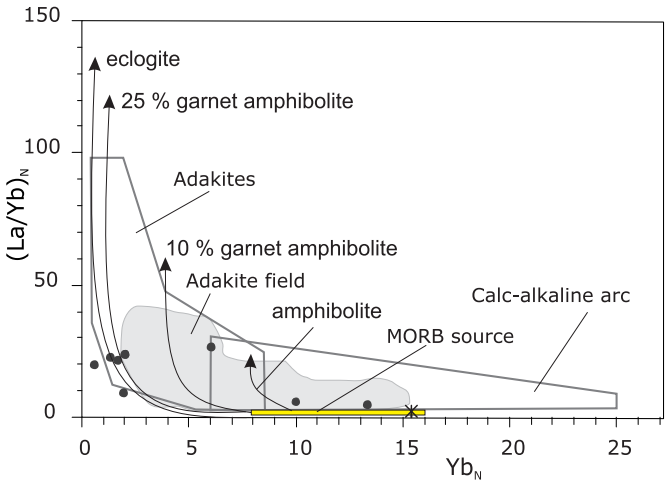

Fig. 12. Diagram $(La/Yb)_N$ vs Yb_N for the Imbicuí Complex rocks in comparison with four partial-melting curves from a mid-ocean basalt (MORB) source (Zhang et al., 2019). Symbols as in Fig. 5.

serpentinites) of the Cerro Mantiqueira Sequence, showing an isotopic composition close to the mantle-derived rocks, with the mafic-ultramafic rocks being enriched, with positive εNd values for all rocks, ranging from + 1 to + 10. In contrast, the Imbicuí and Cambaí complex rocks have an enrichment trend of $^{87}Sr/^{86}Sr_{(740)}$ with values of up to 0.7090 for the Cambaí Complex.

Stevenson et al. (2009) make a discussion correlating Sr/Y and εNd ratios, and in adakite-like samples with the highest εNd values observed to this a least contaminated and have Sr/Y ratios (highest values) reflecting < 30% of the melting. This assumption agrees with the experimental evidence of Rapp et al. (1999), which indicates that high-Al adakite-like suites can be produced by 15–40% partial melting of basalt-like rock compositions. In the Imbicuí Complex, this relationship is similar, with values of $\varepsilon Nd_{(t)}$ of 8.2 and Sr/Y = 170, and $\varepsilon Nd_{(828)}$ of 7.5 and values of 122 ppm, compatible with the interpretation of Stevenson et al. (2009) for melting of basaltic derivation rocks at the origin of the adakites of the Imbicuí Complex.

Neoproterozoic adakites (550 Ma) have been reported in the literature, for example, in the Siberian Craton, the Zimoveyney Massif (Vernikovskaya et al., 2017) suggesting an origin from oceanic crust melting, however, mixed with material from the metasomatized mantle, which would be responsible for the negative $\varepsilon Nd_{(t)}$values, which was not observed in the Imbicuí Complex, where the mantle-derived contribution, primordial or metasomatized, did not play an important role.

In Pb isotopic terms, the $^{206}Pb/^{204}Pb$ and $^{207}Pb/^{204}Pb$ ratios suggest that the rocks of the Imbicuí Complex have a genesis associated with an orogenic environment, plotting with a shift from the mantle evolution curve (Enriched Mantle usually contaminated with lower crust, EM-I). This same behaviour is observed by the similarity of the Cambaí Complex and the amphibolitic rocks of the Cerro Mantiqueira Complex, which suggests a dominant mantle contribution. Still, it does not exclude incipient upper-crust contamination (Enriched Mantle contaminated with the upper crust, EM-II) in their genesis.

Thus, the geochemical characteristics suggest that the adakites of the Imbicuí Complex are associated with the partial melting of the oceanic subduction slab, which was metamorphosed under eclogitic conditions with subordinately slab sediment incorporation. In the Lavras do Sul region, a mafic rock with garnet was described as an eclogite of 903 Ma age (Sue et al., 1992; Pinto et al., 2021) and is suitable to represent the source of adakites of the Imbicuí Complex.

5.4. Age of adakites

Concerning its age, the adakite term was initially defined for Cenozoic rocks (Defant and Drummond, 1990). However, this criterion has not been considered for the use of the term since the chemical characteristics observed in adakites can be obtained from processes that are not directly linked to the age of the rock (Moyen, 2009; Castillo, 2012; Ribeiro et al., 2016).

The calc-alkaline rocks enriched in Na_2O and HSA of the Imbicuí Complex are the leading group (e.g., metatrondhjemite PRE-1A) and can be described as adakitic of Tonian age, with the U–Pb (LA-ICP-MS in zircon) of 828 ± 8 Ma. However, the sample PRE-13I (metagabbro, 845 ± 3 Ma) has a tholeiitic geochemical signature, different in chemical terms compared with adakites, especially in the contents of REE, where it presents a horizontal pattern similar to rocks of the type MORB. An early tholeiitic dominant magmatism in the region, as observed in another Japanese adakitic complex (Yamizo Mountains; Takahashi et al., 2005), may represent the most significant fluid present in the early stages of subduction to produce adakites.

The São Gabriel Terrane presents only the Tonian age described by Leite et al. (1998), with a U–Pb SHRIMP crystallization age of 879 ± 3 Ma for Metadiorito Passinho. Again, the time interval for associating Metadiorito Passinho to the Imbicuí Complex is vast, around 17 Ma if the errors are considered. However, based on the studies by Laux (2017) and Philipp et al. (2018), these rocks are mapped and interpreted as linked to the same magmatism/island arc unit, all with adakite-like rock characteristics. Thus, these ages varying from 879 Ma, 845 Ma, and 828 Ma could be interpreted as i) incremental batches generated in the same protracted island arc or ii) a generation interval of different island arcs amalgamated with the closure of the Charrua Ocean.

Discussing the three ages for the rocks of the Imbicuí Complex, the presence of a population of zircons inherited from about 920 Ma occurs only in the sample (PRE-1A), suggesting: i) participation of an older oceanic crust in the generation of these rocks, or ii) the presence of zircons of that age in sediments incorporated during oceanic slab melting. Also, no Paleoproterozoic contribution in the zircon ages was characterized until now, precluding an "older" than 920 Ma crustal component in its evolution and adding another evidence to the juvenile magmatic character of these rocks.

The Imbicuí Complex evolution in the São Gabriel Terrane can be explained by the subduction of the Charrua Ocean (Fragoso-César et al., 1986) underneath the Nico Perez Terrane (Paleoproterozoic crust; Philipp et al., 2018) or below Arachania (Encantadas) Microplate (Paleoproterozoic crust; Ramos et al., 2017). The closure of the Charrua Ocean generated the subduction of the oceanic intra arc (island arc), where incremental melting events were responsible for the evolution of the juvenile arc – Passinho Arc (Hartmann et al., 2000) – beginning at 879 Ma (Passinho Metadiorite) followed by a tholeiitic at 845 Ma to metatrondhjemitic calc-alkaline (low-K) magmatism at 828 Main the Imbicuí Complex (Fig. 13). Thus, the rock complexity can be explained by the high rate geodynamics hot subducted and extruded oceanic crust in an island arc setting.

6. Conclusions

The dioritic-tonalitic-trondhjemitic rocks of the Imbicuí Complex show characteristics similar to adakites, as observed by the high Sr/Y (~100) and La/Yb (~25) ratios. Adakite rocks in the region present calc-alkaline affinity with an age of 828 Ma, and subordinately the tholeiitic rocks present a crystallization age of 845 Ma. The adakites are classified as high-SiO_2 (> 63%) and Type 1, with relative enrichment in Al_2O_3, and Na_2O, associated with low values of K_2O and MgO.

The source for these adakites suggests oceanic crust melting, probably eclogitic, with little mantle involvement in its genesis (low Mg#, $\varepsilon Nd_{(828)}$ positive). The values of $^{87}Sr/^{86}Sr_{(i)}$ suggest a MORB-like component (0.704) and a sedimentary component (0.709) in the origin of the Imbicuí Complex adakites which is also observed with the presence of circa 920 Ma inherited zircons. The $\varepsilon Nd_{(828)}$ (+8.2 to + 7.5) and model ages Nd-T_{DM} of 0.8 and 0.9 Ga (similar to the age of

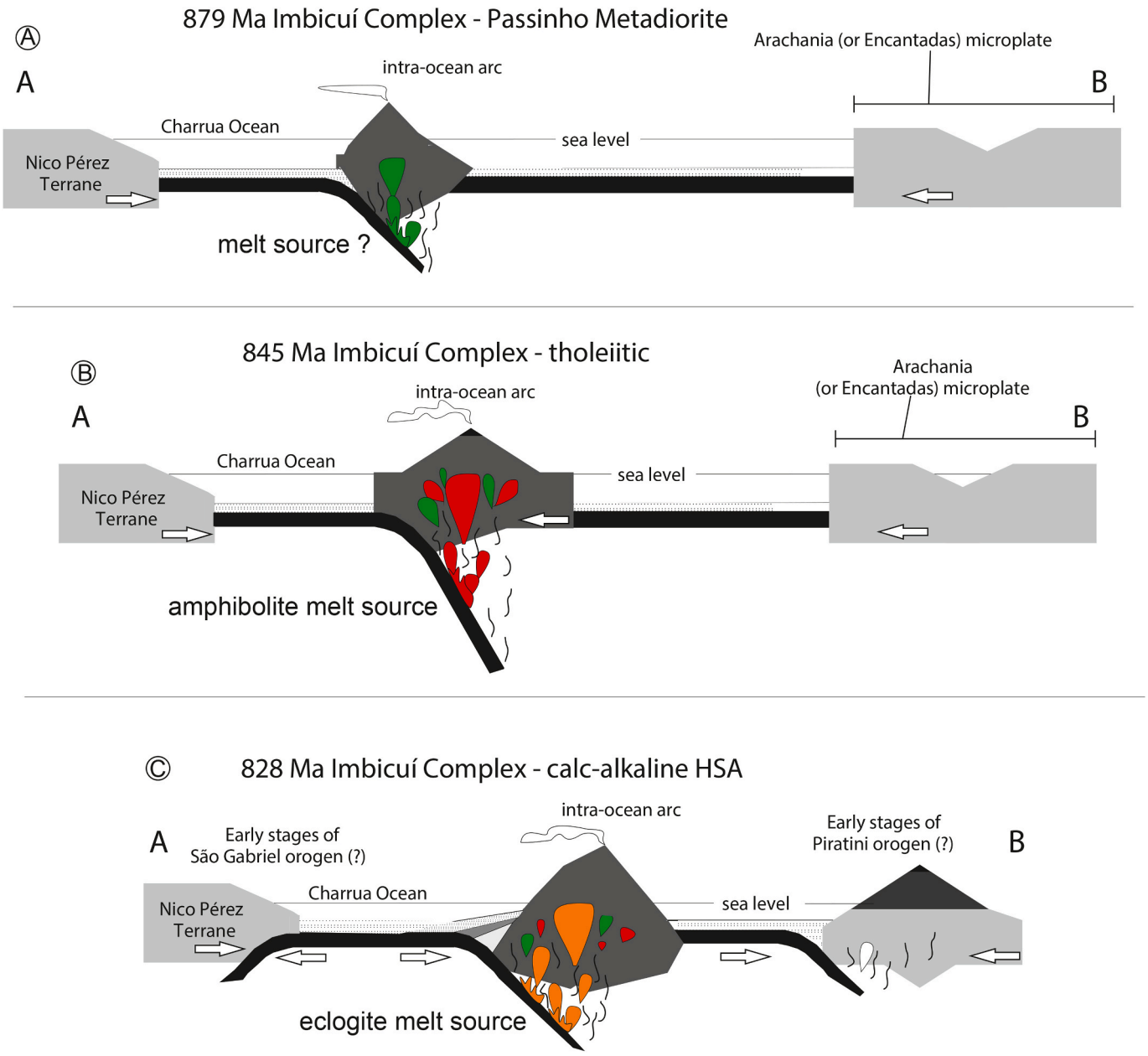

Fig. 13. Schematic model, not in scale, for the evolution of Imbicuí Complex, São Gabriel Terrane, Dom Feliciano Belt. A) 879 Ma and the generation of the Metadiorite Passinho (Leite et al., 1998); B) 845 Ma and the generation of the tholeiitic rock of Imbicuí Complex; C) 828 Ma and the generation of the calc-alkaline HSA of Imbicuí Complex and the initial stages (?) of São Gabriel Orogeny (Hartmann et al., 2000) and Piratini Orogeny (Vieira et al., 2019).

crystallization) suggest that these rocks represent juvenile magmatism generated in an orogenic environment (ratios $^{206}Pb/^{204}Pb$ and $^{207}Pb/^{204}Pb$, 17.70 to 18.40 and 15.49 and 15.55) of an island arc.

In its initial phase, this arc produces magmas with the release of plate fluids and generation of low-deepness tholeiitic magmatic affinity with amphibolite as the main source and, subsequently, the high-deepness adakitic calc-alkaline rocks with eclogite as the main source.

The subduction of an intra-oceanic arc linked to the Charrua Ocean, and orogenic metamorphism of the oceanic crust, combined with the participation of sediments, produced adakite-like rocks of the Imbicuí Complex, São Gabriel Terrane, Dom Feliciano Belt.

Funding

This work was supported by the Fundação de Apoio a Pesquisa no Rio Grande do Sul (FAPERGS) [grant number 19/2551-0001774-0] and the Conselho Nacional de Desenvolvimento Científico e Tecnológico (CNPq) [grant number 314501/2020–7].

CRediT authorship contribution statement

Rosemeri Soares Siviero: Writing – original draft, Visualization, Methodology, Investigation, Formal analysis, Data curation, Conceptualization. **Edinei Koester:** Writing – original draft, Funding acquisition, Formal analysis, Data curation, Conceptualization. **Luis Alberto Dávila Fernandes:** Writing – original draft, Investigation, Funding acquisition, Conceptualization. **Delphine Bosch:** Validation, Supervision, Methodology, Investigation. **Olivier Bruguier:** Validation, Supervision, Methodology, Investigation. **Daniel Triboli Vieira:** Methodology, Investigation, Formal analysis. **Rodrigo Chaves Ramos:** Methodology, Investigation, Formal analysis. **Gustavo Kraemer:** Investigation, Conceptualization.

Declaration of competing interest

The authors declare the following financial interests/personal relationships which may be considered as potential competing interests: Edinei Koester reports financial support was provided by Conselho Nacional de Desenvolvimento Científico e Tecnológico and also by Fundação de Apoio a Pesquisa no Rio Grande do Sul.

Data availability

Data will be made available on request.

Acknowledgements

The authors thank the Institute of Geosciences of UFRGS for technical and infrastructure support. We thank Research Support Foundation in Rio Grande do Sul (FAPERGS), National Council for Scientific and Technological Development (CNPq) for financial support, and J.H. for English improvement in the text. This manuscript has significantly benefitted from the contributions of two anonymous reviewers and the editorial handling by Dr. Veronica Oliveros.

Appendix A. Supplementary data

Supplementary data to this article can be found online at https://doi.org/10.1016/j.jsames.2023.104545.

References

Almeida, F.F.M., Hasui, Y., Brito-Neves, B.B., Fuck, R.A., 1981. Brazilian structural provinces: an introduction. Earth Sci. Rev. 17, 1–29.
Arena, K., Hartmann, L.A., Lana, C., 2016. Evolution of Neoproterozoic ophiolites from the southern Brasiliano Orogen revealed by zircon U-Pb-Hf isotopes and geochemistry. Precambrian Res. 285, 299–314.
Atherton, M.P., Petford, N., 1993. Generation of sodium-rich magmas from newly underplated basaltic crust. Nature 362, 144–146.
Babinski, M., Chemale Jr., F., Hartmann, L.A., Van Schmus, W.R., Silva, L.C., 1996. Juvenile accretion at 750-700 Ma in southern Brazil. Geology 24 (5), 439–442.
Barker, F., 1979. Trondhjemite: definition, environment and hypotheses of origin. In: Baker, F. (Ed.), Trondhjemites, Dacites and Related Rocks. Elsevier, Amsterdam-Oxford-New York, pp. 1–12.
Bastos, V.A., Koester, E., Lenz, C., Dal Olmo-Barbosa, L., Porcher, C.C., Loureiro, P.O., Vieira, D.T., Ramos, R.C., Cedeño, D.G., 2020. Contributions to the understanding of the Pinheiro Machado Complex (Dom Feliciano Belt, Brazil) through study of textures, mineral chemistry and crystallization conditions. Geol. J. https://doi.org/10.1002/gj.3980.
Bebout, G., Ryan, J.G., Leeman, W.P., Bebout, A.E., 1999. Fractionation of trace elements during subduction-zone metamorphism: effect of convergent margin thermal evolution. Earth Planet Sci. Lett. 171, 63–81.
Blichert-Toft, J., Zanda, B., Ebel, D.S., Albarède, F., 2010. The solar system primordial lead. Earth Planet Sci. Lett. 300 (1–2), 152–163.
Castillo, P.R., 2012. Adakite petrogenesis. Lithos 134–135, 304–316.
Condie, K.C., 2005. TTGs and adakites: are they both slab melts? Lithos 80, 33–44.
Corfu, F., Hanchar, J.M., Hoskin, P.W.O., Kinny, P., 2003. Atlas of zircon textures. Rev. Mineral. Geochem. 53, 469–500.
Defant, M.J., Drummond, M.S., 1990. Derivation of Some Modern Arc Magmas by Melting of Young Subducted Lithosphere. Nature 347, pp. 662–665.
Defant, M.J., Kepezhinskas, P., 2001. Evidence suggests slab melting in arc magmas. In: Eos, Transactions, vol. 82. Amer.Geoph. Union, pp. 65–69.
Defant, M.J., Jackson, T.E., Drummond, M.S., Boer, J.Z., Bellon, H., Feigenson, M.D., Maury, R.C., Stewart, R.H., 1992. The geochemistry of young volcanism throughout western Panama and southeastern Costa Rica: an overview. J. Geol. Soc. 149, 569–579.
Defant, M.J., Xu, J.F., Kepezhinskas, P., Wang, Q., Zhang, Q., Xiao, L., 2012. Adakites: some variations on a theme. Acta Petrol. Sin. 18, 129–142.
DePaolo, D.J., 1981. Trace element and isotopic effects of combined wall-rock assimilation and fractional crystallization. Earth and Planetary Science Letters 53, 189–202.
Drummond, M.S., Defant, M.J., 1990. A model for trondhjemite-tonalite-dacite genesis and crustal growth via slab melting: Archean to modern comparisons. J. Geophy. Res. 95, 205–215.
Faure, G., Mensing, T.M., 2005. Isotopes: Principles and Applications, third ed. John Wiley & Sons, Nova Jersey, p. 523.
Fragoso-César, A.R.S., Figueiredo, M.C.H., Soliani Jr., E., Faccini, U.F., 1986. O batólito Pelotas (proterozóico superior/eo-paleozóico) no Escudo do Rio Grande do Sul. XXXIV Congresso Brasileiro de Geologia, Goiânia, Annals 3, 1322–1343.
Gill, R., 2010. Igneous Rocks and Processes. A Practical Guide. Willey-Blackwell, UK, p. 428p.
Gomez-Tuena, A., LaGatta, A., Langmuir, C., Goldstein, S., Ortega-Gutierrez, S., Carrasco-Nunez, G., 2003. Temporal control of subduction magmatism in the eastern Trans-Mexican Volcanic Belt: mantle sources, slab contributions and crustal contamination. Geochem. Geophy. Geosys. 4 https://doi.org/10.1029/2003GC000524.
Girelli, T.J., Chemale, F., Lavina, E.L.C., Laux, J.H., Bongiolo, E.M., Lana, C., 2018. Granulite accretion to Rio de la Plata Craton, based on zircon U-Pb-Hf isotopes: tectonic implications for Columbia Supercontinent reconstruction. Gondwana Res. 56, 105–118.
Hartmann, L.A., Leite, J.A.D., Silva, L.C., Remus, M.V.D., McNaughton, N.J., Groves, D.I., Fletcher, I.R., Santos, J.O.S., Vasconcellos, M.A.Z., 2000. Advances in SHRIMP geochronology and their impact on understanding the tectonic and metallogenic evolution of southern Brazil. Austral. J. Earth Sci. 47 (5), 829–844.
Hartmann, L.A., Philipp, R.P., Santos, J.O.S., McNaughton, N.J., 2011. Time frame of 753–680 Ma juvenile accretion during the São Gabriel orogeny, southern Brazilian Shield. Gondwana Res. 19, 84–99.
Hartmann, L.A., Werle, M., Michelin, C.R.L., Lana, C., Queiroga, G.N., Castro, M.P., Arena, K.R., 2019. Proto-Adamastor ocean crust (920 Ma) described in Brasiliano Orogen from coetaneous zircon and tourmaline. Geosci. Front. 10 (4), 1623–1633.
Heilbron, M., Valeriano, C.M., Peixoto, C., Tupinambá, M., Neubauer, F., Dussin, I., Corrales, F., Bruno, H., Lobato, M., Almeida, J.C.H., Silva, L.G.E., 2020. Neoproterozoic magmatic arc systems of the central Ribeira belt, SE-Brazil, in the context of the West-Gondwana pre-collisional history: a review. J. South Amer. Earth Sci. 103, 102710.
Hueck, M., Oyhantçabal, P., Philipp, R.P., Basei, M.A.S., Siegesmund, S., 2018. The Dom Feliciano belt in southern Brazil and Uruguay. In: Siegesmund, S., Basei, M., Oyhantçabal, P., Oriolo, S. (Eds.), Geology of Southwest Gondwana. Springer, Regional Geology Reviews, pp. 267–302.
Janoušek, V., Farrow, C.M., Erban, V., 2006. Interpretation of whole-rock geochemical data in igneous geochemistry: introducing Geochemical Data Toolkit (GCDkit). J. Petrol. 47 (6), 1255–1259.
Jégo, S., Maury, R.C., Polve, M., Yumul Bellon, H., Tamayo, R.A., Cotton, J., 2005. Geochemistry of adakites from the Philippines: constraints on their origins. Resour. Geol. 55 (3), 163–187.
Kimura, J.I., Gill, J.B., Kunikiyo, T., Osaka, I., Shimoshioiri, Y., Katakuse, M., Kakubushi, S., Nagao, T., Furuyama, K., Kamei, A., Kawabata, H., Nakajima, J., Van Keken, P., Stern, R.J., 2014. Diverse magamtic effects of subducting a hot slab in SW Japan: Results from a forward modeling. Geochem. Geophy. Geosys. 15 (3), 691–739.
Kraemer, G., 1995. Evolução magmática e tectônica da Suíte OrtometamórficaImbicuí, região de Lavras do Sul (RS). Dissertação de mestrado - Instituto de Geociências, Universidade Federal do Rio Grande do Sul, Porto Alegre, p. 99.
Laux, J.H., 2017. Geologia e recursos minerais da Folha Lagoa da Meia-Lua – SH. 21-Z-B-VI, Escala 1:100.000. Porto Alegre. CPRM, 2017. 255pp.
Lebedev, V.A., Vashakidze, G.T., Parfenov, A.V., Yakushev, A.I., 2019. The origin of adakite-like magmas in the modern continental collision zone: evidence from pliocene dacitic volcanism of the akhalkalaki lava plateau (Javakheti Highland, lesser caucasus). Petrology 27 (3), 307–327.
Leite, J.A.D., Hartmann, L.A., McNaugton, N.J., Chemale Jr., F., 1998. SHRIMP U/PB zircon geochronology of Neoproterozoic juvenile and crustal-reworked terranes in southernmost Brazil. Int. Geol. Rev. 40, 688–705.
Loureiro, P.O., Koester, E., Weinberg, R., Porcher, C.C., Lenz, C., Ramos, R.C., Vieira, D. T., Bastos, V.A., Knijinick, D., Pimentel, M.M., 2021. Recycling and hybridization of incremental episodes of magma intrusions: Pinheiro Machado Complex, southeastern Dom Feliciano Belt, Brazil. J. South Amer. Earth Sci. 105, 102922.
Ludwig, K.R., 2003. Isoplot 3.0 – a geochronological toolkit for microsoft excel. In: Berkley Geochronology Center, Special Publication, 4.
Maniar, P.D., Piccoli, P.M., 1989. Tectonic discriminations of granitoids. Geol. Soc. Am. Bull. 101, 635–643.
Martin, H., 1986. Effect of steeper Archaean geothermal gradient on geochemistry of subduction zone magmas. Geology 14, 753–756.
Martin, H., 1999. Adakitic magmas: modern analogs of Archaean granitoids. Lithos 46, 411–429.
Martin, H., Smithies, R.H., Rapp, R., Moyen, J.-F., Champion, D., 2005. An overview of adakite, tonalite-trondhjemite-granodiorite (TTG), and sanukitoid: relationships and some implications for crustal evolution. Lithos 79, 1–24.
Masquelin, H., Fernandes, L.A.D., Lenz, C., Porcher, C.C., McNaughton, N.J., 2012. The Cerro Olivo Complex: a pre-collisional neoproterozoic magmatic arc in eastern Uruguay. Int. Geol. Rev. 54 (10), 1161–1183.
Middelmost, E.A., 1994. Naming materials in the magma/igneous rocks system. Earth Sci. Rev. 37, 215–224.
Moyen, J.-F., 2009. High Sr/Y and La/Yb ratios: the meaning of the “adakitic signature”. Lihtos 112 (3–4), 556–574.
Naqvi, S.M., Prathap, J.G.R., 2007. Geochemistry of adakites from Neoarchean active continental margin of Shimoga schist belt, Wester Dharwar Craton, India: implications for the genesis of TTG. Prec. Res. 156 (1), 32–54.
Philipp, R.P., Pimentel, M.M., Chemale Jr., F., 2016. Tectonic evolution of the Dom Feliciano Belt in southern Brazil: geological relationships and U-Pb geochronology. Brazil. J. Geol. 46 (1), 83–104.
Philipp, R.P., Pimentel, M.M., Chemale Jr., F., 2018. Tectonic evolution of the Dom Feliciano Belt in southern Brazil: geological relationships and U-Pb geochronology. Brazil. J. Geol. 46 (1), 83–104.
Pinto, V.M., Debruyne, D., Hartmann, L.A., Queiroga, G.N., Lana, C., Fragoso, B.A.M., Porcher, C.C., Castro, M.P., Laux, J., 2021. Metamorphic evolution of a Tonian

eclogite associated with an island arc of the southern Brasiliano Orogen. Precambrian Res. 366, 106414.
Ramos, R.C., Koester, E., Vieira, D.T., 2020. Sm–Nd systematics of metaultramafic-mafic rocks from the Arroio Grande Ophiolite (Brazil): insights on the evolution of the South Adamastor paleo-ocean. Geosci. Front. https://doi.org/10.1016/j.gsf.2020.02.013.
Pyle, D.G., Christie, D.M., Mahoney, J.J., 1992. Resolving an isotopic boundary within the Australian-Antartic discordance. Earth Plan. Sci. Let. 112 (1–4), 161–178.
Ramos, R.C., Koester, E., Porcher, C.C., 2017. Chemistry of chromites from Arroio Grande ophiolite (Dom Feliciano Belt, Brazil) and their possible connection with the nama group (Namibia). J. South Amer. Earth Sci. 80, 192–206.
Ramos, R.C., Koester, E., Vieira, D.T., Porcher, C.C., Gezatt, J., Silveira, R., 2018. Insights on the evolution of the Arroio Grande ophiolite (Dom Feliciano belt, Brazil) from Rb-Sr and SHRIMP U-Pb isotopic geochemistry. J. South Amer. Earth Sci. 86, 38–53.
Rapp, N., Shimizu, N., Norman, M.D., Apllegate, J.S., 1999. Reaction between slab-derived and peridotite in the mantle wedge: experimental constraints at 3.8 GPa. Chem. Geol. 160, 335–356.
Rapp, R.P., Shimizu, N., Norman, M.D., Applepate, G.S., 1999. Reaction between slab-derived melts and peridotite in the mantle wedge: experimental constraints at 3.8 GPa. Chem. Geol. 160, 335–356.
Ribeiro, J.M., Maury, R.C., Grégoire, M., 2016. Are adakites slab melts or high-pressure fractionated mantle melts ? J. Petrol. 57 (5), 839–862.
Rollinson, H., 1993. Using Geochemical Data: Evaluation, Presentation, Interpretation. Longman, Harlow, p. 352.
Saalmann, K., Gerdes, A., Lahaye, Y., Hartmann, L.A., Remus, M.V.D., Läufer, A., 2011. Multiple accretion at the eastern margin of the Rio de la Plata craton: the prolonged Brasiliano orogeny in southernmost Brazil. Int. J. Earth Sci. 100, 355–378.
Saalmann, K., Hartmann, L.A., Remus, M.V.D., Koester, E., Conceição, R.V., 2005a. Sm-Nd isotope geochemistry of metamorphic volcano-sedimentary successions in the São Gabriel Block, southernmost Brazil: evidence for the existence of juvenile Neoproterozoic oceanic crust to east of the Rio de la Plata Craton. Precambrian Res. 136, 159–175.
Saalmann, K., Remus, M.V.D., Hartmann, L.A., 2005b. Geochemistry and crustal evolution of volcano-sedimentary succession and orthogneisses in the São Gabriel block, southernmost Brazil- relics of neoproterozoic magmatic arcs. Gondwana Res. 8 (2), 143–161.
Shand, S.J., 1943. Eruptive Rocks: Their Genesis, Composition, Classification, and Their Relation to Ore-Deposits with a Chapter on Meteorite. Hafner Publishing, New York.
Siviero, R.S., Bruguier, O., Fernandes, L.A.D., Koester, E., Porcher, C.C., Kraemer, G., 2021. Ages and geochemistry of Cambaí complex, São Gabriel terrane, Brazil: arc-related TTG-like rocks. J. South Amer. Earth Sci. 108, 103165.
Siviero, R.S., Fernandes, L.A.D., Koester, E., Jourdan, F., 2022. Tonian and cryogenian 40Ar/39Ar hornblende and muscovite ages for the São Gabriel terrane, Dom Feliciano belt, southern Brazil. Geol. J. 57, 1137–1152.
Stevenson, R.K., Henry, P., Gariepy, C., 2009. Isotopic and geochemical evidence for differentiation and crustal contamination from granitoids of the Berens river subprovince, Superior province, Canada. Precambrian Res. 168, 123–133.
Sue, R.B., Goffermann, M., Pinto, R.F., Xavier, F.F., 1992. Ocorrência de eclogitos no Escudo Sul-rio-grandense: dados preliminares. 37o Congresso Brasileiro de Geologia, São Paulo, SP, Resumos. SBG, 1p.
Sun, S.S., McDonough, W.F., 1989. Chemical and isotopic systematics of oceanic basalt: implications for mantle composition and processes. Geol. Soc. Spec. Publ. 42, 313–345.
Takahashi, Y., Kagashima, S., Mikoshiba, M.U., 2005. Geochemistry of adakitic quartz diorite in the Yamizo Mountains, central Japan: implications for Early Cretaceous adakitic magmatism in the inner zone of southwest Japan. Isl. Arc 14, 150–164.
UFRGS, 1991. Mapeamento geológico 1:25.000 de parte da Folha Lavras do. Universidade Federal do Rio Grande do Sul. Sul (MI2995/3) e de parte da Folha de Coxilha do Tabuleiro (MI2994/4): Projeto Lavras do Sul e Coxilha do Tabuleiro. – Trabalho de graduação em geologia.
UFRGS, 2004. Mapeamento geológico 1:25.000 de parte da Folha Lavras do. Universidade Federal do Rio Grande do Sul. Sul (MI2995/3): Projeto Lavras do Sul. Trabalho de Graduação em geologia.
UFRGS, 2005. Mapeamento geológico 1:25.000 de parte da Folha de Coxilha do Tabuleiro (MI2994/4): Projeto Coxilha do Tabuleiro. Trabalho de Graduação em geologia. Universidade Federal do Rio Grande do Sul.
Vieira, D.T., Koester, E., Ramos, R.C., Porcher, C.C., 2019. Sr-Nd-Hf isotopic constraints and U-Pb geochronology of the ArroioPedrado Gneisses, Dom Feliciano Belt, Brazil: a 680 Ma shoshonitic event in the final stages of the Piratini Arc evolution. J. South Amer. Earth Sci. 95, 102294.
Vernikovskaya, A.E., Matushkina, N.Y., Kadilnikova, P.I., Romanov, I.V., Larionovc, A. N., 2017. Adakite-gabbro-anorthosite magmatism at the final (576–546 Ma) development stage of the neoproterozoic active margin in the South-west of the siberian Craton1. Dok. Earth Sci. 477 (2), 1402–1407.
Weiss, Y., Class, C., Goldstein, S.L., Hanyu, T., 2016. Key new pieces of the HIMU puzzle from olivines and diamond inclusions. Nature 537, 666–670.
Wiedenbeck, M., Allé, P., Corfu, F., Griffin, W.L., Meier, M., Oberli, F., Von Quadt, A., Roddick, J.C., Spiegel, W., 1995. Three natural zircon standards for U-Th-Pb, Lu-Hf, trace element and REE analyses. Geostand. Newsl. 19, 1–23.
Yumul Jr., G.P., Dimalanta, C.B., Bellon, H., Faustino, D.V., De Jesus, J.V., Tamayo Jr., R. A., Jumawan, F.T., 2000. Adakitic lavas in the Central Luzon back-arc region, Philippines: lower crust partial melting products? Isl. Arc 9, 499–512.
Zhang, L., Li, S., Zhao, Q., 2019. A review of research on adakites. Int. Geol. Rev. https://doi.org/10.1080/00206814.2019.1702592.
Zhang, H., Niu, H., Sato, H., Yu, X., Shan, Q., Zhang, B., Ito, J., Nagao, T., 2005. Late paleozoic adakites and Nb-enriched basalts from northern Xinjiang, northwest China: evidence for the southward subduction of the paleo-asian oceanic plate. Isl. Arc 14, 55–68.
Zindler, A., Hart, S., 1986. Chemical geodynamics. Annu. Rev. Earth Planet Sci. 14, 493–571.